AD-A039 239 AIR FORCE INST OF TECH WRIGHT-PATTERSON AFB OHIO SCH--ETC F/G 21/5
EXPLODING WIRE SIMULATION OF JET-ENGINE GAS-PATH MICRODISTRESSE--ETC(U)
DEC 75 J E MITCHELL

UNCLASSIFIED AFIT/GNE/PH/75-20 NL

| OF |
AD
A039239

END

DATE
FILMED
5-77

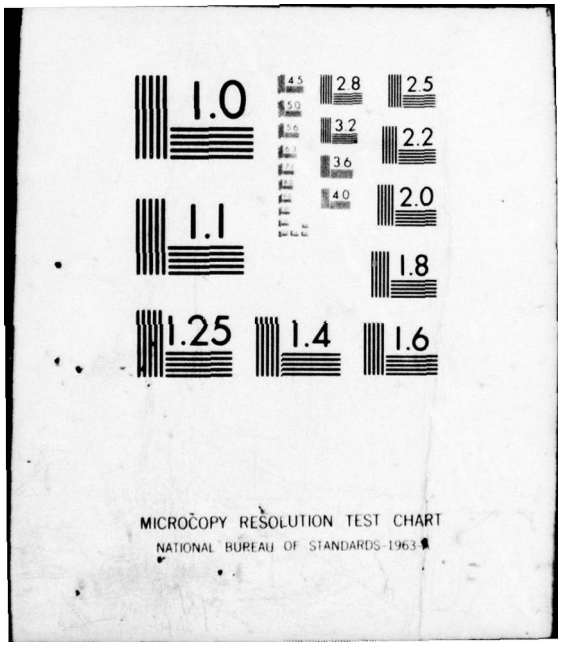
1.0
1.1
1.25
1.4
1.6
1.8
2.0
2.2
2.5
2.8
3.2
3.6
4.0
4.5
5.0
MICROCOPY RESOLUTION TEST CHART
NATIONAL BUREAU OF STANDARDS-1963-A

GNE/PH/75-20

B.S.

EXPLODING WIRE SIMULATION OF JET-ENGINE GAS-PATH MICRODISTRESSES

THESIS

GNE/PH/75-20

John E. Mitchell
Major USAF

(14) AFIT/GNE/PH/75-20

(6)

EXPLODING WIRE SIMULATION OF JET-ENGINE GAS-PATH MICRODISTRESSES.

(9) Master's THESIS,

Presented to the Faculty of the School of Engineering

of the Air Force Institute of Technology

Air University,

in Partial Fulfillment of the

Requirements for the Degree of

Master of Science

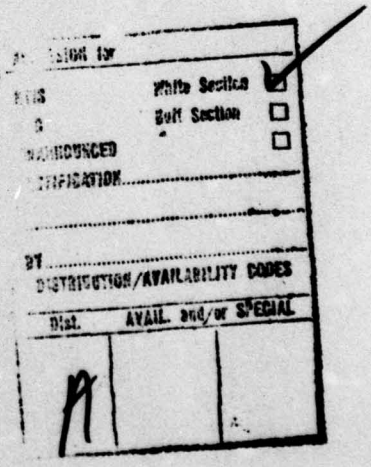

by

(10) John E. Mitchell, B.S.

Major USAF

Graduate Nuclear Engineering

(11) Dec[redacted]75

(12) 68 p.

Approved for public release; distribution unlimited.

012 225

1473

Preface

GNE/PH/75-20

This thesis was sponsored by the Air Force Flight Dynamics Laboratory (AFFDL). It is part of a continuing effort to develop a feasible engine-failure warning system based on the detection of boluses of charge in the engine exhaust of jet engines. Such a warning system could result in a dramatic reduction in jet aircraft accident rates, especially single-engine aircraft rates since this system could predict a catastrophic engine failure hours ahead of its actual occurrence. The development effort has been hindered, however, by the lack of a proven theory of bolus formation and an uncertainty as to the precise meaning of data gathered with ion probes. It is sincerely hoped that this work will illuminate both of these areas.

I would like to express my deep appreciation to my thesis advisor, Major Robert P. Couch, who has given invaluable advice and assistance. His ingenuous equipment design and concepts were invaluable in making the discoveries which are reported in this thesis. He was the originator of the designs for the particle separator and the Gaussian cylinder which were keys to the success of this research.

Additionally, I would like to thank my son and my wife for their understanding and acceptance of the time and attention that I could not give to them. And finally, a note of appreciation is due to Mrs. Van Hoang for the moral support of her and her four children, Vietnamese refugees, who I have sponsored during this period of work.

Contents

Contents

List of Figures

List of Figures

List of Tables

Abstract

Exploding wires were used to simulate jet-engine gas-path microdistresses. The physical processes involved in the formation of boluses of charge in a flowstream were investigated and the amounts of bolus charge produced under various conditions were measured. Ion-probe responses were concurrently recorded. The results of the investigation were used to construct a theory of bolus formation.

Large negative boluses of charge were produced by the injection of hot metal particles into a flowstream. Smaller positive boluses were produced by heating a wire to a temperature near its melting point. Ion-probe responses were shown to be very misleading when used as a sole source of information as to the charge in a bolus. It is recommended that immediate attention be given to the detection of negative boluses of charge in a jet engine exhaust since negative boluses would most probably be produced by the more severe (very hot particles) microdistress which could lead to catastrophic engine failure.

EXPLODING WIRE SIMULATION OF JET-ENGINE GAS-PATH MICRODISTRESSES

I. Introduction

Background

A gas-path microdistress is defined as any localized event along the gas-path of a jet engine that causes any combination of hot metal particles, metal ions, free electrons, and/or plasma to be injected into the flowstream. An example of a microdistress would be a rubbing turbine-blade tip or a hot spot in a burner can. Although a microdistress is initially localized, it can increase in severity with engine operation time and eventually result in either component failure or catastrophic engine failure. It has been found that microdistresses cause the formation of boluses of charge in the exhaust of a jet engine.

The prediction of impending jet-engine gas-path failures by the detection and interpretation of these boluses of charge has received increasing interest during the past five years. The first recorded observation that made this possibility manifest occurred on November 17, 1970 (Ref 2:2). Captain Robert Vopalensky, while taking current-voltage traces from a probe inserted into the exhaust of a jet engine in order to determine plasma density, noted the appearance of some large-amplitude spikes on his traces. The number of spikes observed per unit time increased with each succeeding measurement throughout the day. On

the following day, a second-stage turbine blade experienced a fatigue failure (Ref 3:516-517).

Since this observation, a number of investigations of the phenomenon have taken place. The Air Force Aero Propulsion Laboratory (AFAPL) has published seven technical reports on the subject, the Air Force Flight Dynamics Laboratory two, and the Air Force Avionics Laboratory one (Ref 8:3-10). Additionally, there have been four related masters theses (Ref 3, 4, 7, 9) authored by past students of the Air Force Institute of Technology and a fifth one (Ref 1) which is concurrently being written with this thesis. However, it is the conclusion of the authors of the most recent AFAPL report that the electrostatic (ion) probe technique for the prediction of jet-engine failures has not yet demonstrated the effectiveness or reliability necessary for advanced development (Ref 8:17). This conclusion was reached because of inconsistencies in engine test results and an inability to either develop a consistent theory of probe operation or to identify probe signal types.

More basic to the problem, however, is both the lack of a clear determination of bolus composition and the lack of a proven theory of bolus formation. It is not known with certainty whether the engine-exhaust boluses which are being detected are composed of particles, ions, or combinations of the two. And since the response of an ion probe is different in each case, there will probably continue to be inconsistencies in engine test data until the question of composition is resolved. But even if engine test results can be shown to be consistent,

a proven theory of bolus formation is needed before the ion-probe technique can be selectively predictive in distinguishing between different types of gas-path component failures.

Purpose

The purpose of this thesis is to develop a theory of bolus formation and to demonstrate the varying responses of ion probes to boluses of different composition. It is intended to augment current jet-engine field investigations with results obtained under controlled laboratory conditions. Hopefully, these results will lead to a better understanding of the bolus-formation phenomenon and a clearer insight of how to use this phenomenon to predict jet engine failures.

Approach

Exploding wires were used for the simulation of jet-engine gas-path microdistresses. This simulation was used to investigate the physical processes involved in bolus formation and to measure the amounts of bolus charge produced under various conditions. Ion-probe responses were concurrently recorded. The results of the investigation were then used to construct a theory of bolus formation, and they form the basis for recommended changes to current jet-engine ion-probe investigation techniques.

Organization

This thesis is an experimental thesis. Therefore, the equipment which was used will first be described in detail. A theory chapter

follows the equipment description. Although it is titled Theory, Chapter III contains both theory and explanation because the detailed discussion of the topics it contains is a necessary prerequisite for the complete comprehension of the chapter that follows which contains the experimental results.

Chapter IV contains a detailed account of the experimental results which lead to the formulation of a theory of negative bolus formation. It also discusses ion-probe responses and measurement of bolus charge. An evaluation is made of the thermionic-emission model which is proposed to explain how particles become positively charged. In the last chapter, the conclusions are summarized and recommendations are made.

II. Equipment

The purpose of this section is to provide a detailed description of the construction and operation of the laboratory equipment. The three types of equipment employed, categorized by usage, are the flowstream components, the exploding wire circuit elements, and the measurement equipment. Fig. 1, page 6, is a photograph of the flowstream components and capacitive discharge circuit.

Flowstream Components

The three main flowstream components, shown in Fig. 2, page 7, are the exploding-wire chamber, the particle separator, and the Gaussian cylinder. Pressurized air is supplied by a Worthington type-YB-2 feather-valve compressor capable of delivering 100 psi at a 500-cfm flow rate. It is fitted with a Lectrodryer type-BZ electric dryer. The air is filtered with a 0.90-micron-pore paper filter just prior to entering the stagnation chamber. Air pressure in the stagnation chamber is measured by a mercury manometer. After leaving the stagnation chamber the air flows through the exploding-wire chamber, the particle separator, and the Gaussian cylinder in that order. The sections are connected with 2-in. pieces of rubber hose and metal clamps and are electrically isolated from each other.

The purpose of the exploding-wire chamber is to inject a pocket of hot metal particles, ions, and plasma into the flowstream. This pocket then flows through the particle separator which electrically discharges

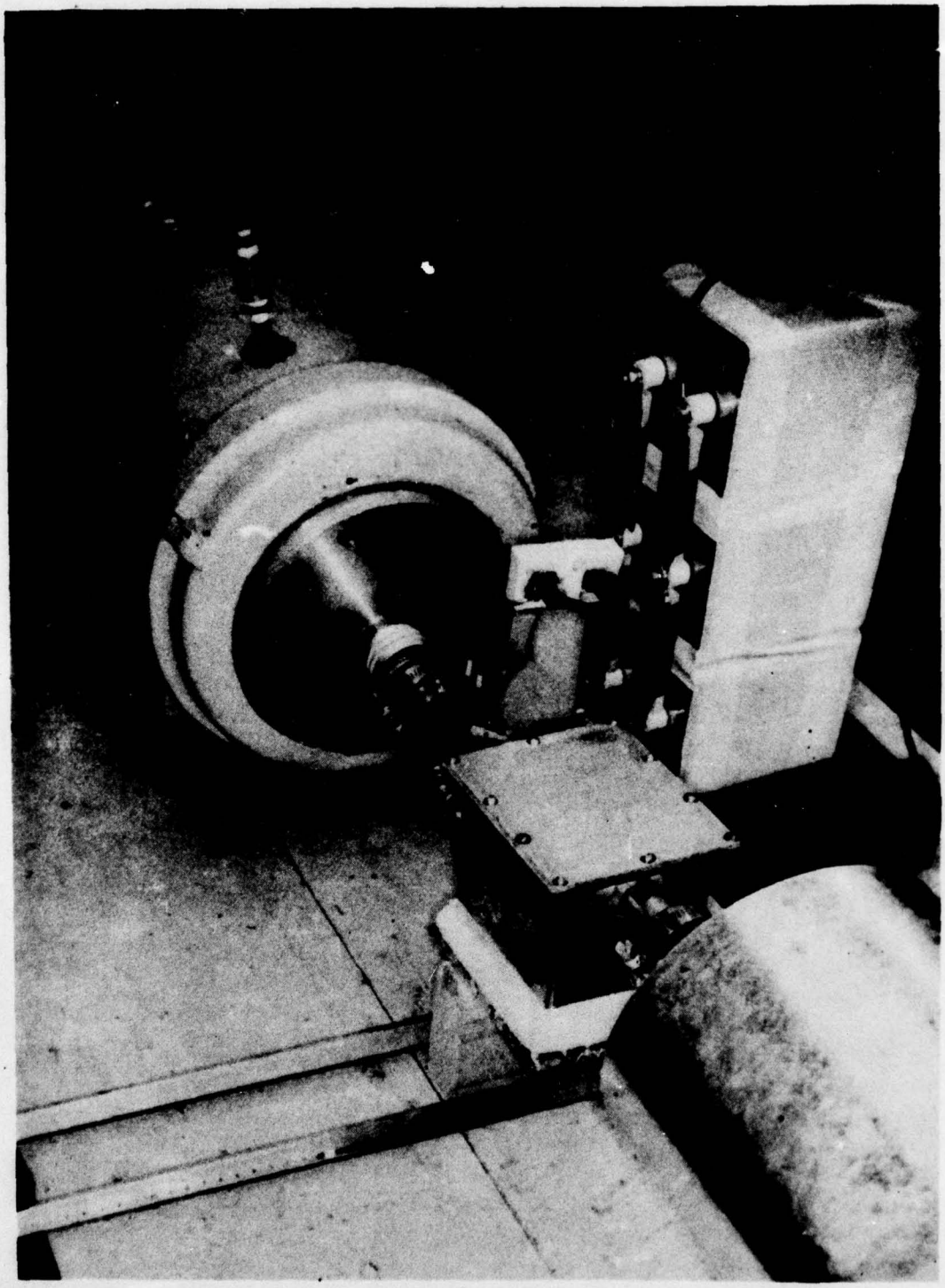

Fig. 1 Flowstream Components and Capacitive Discharge Circuit

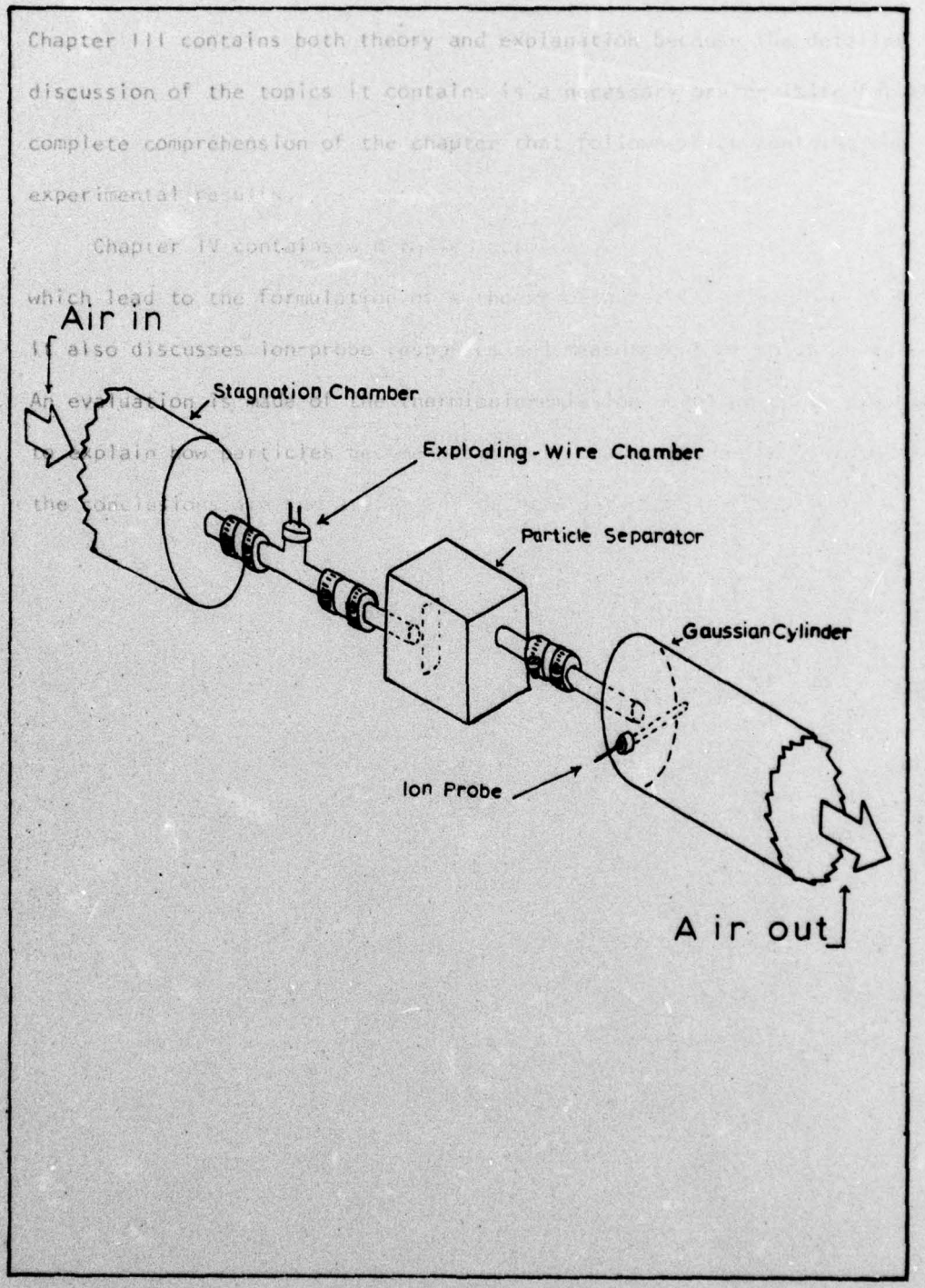

Fig. 2 Flowstream Components

and separates particles. The Gaussian cylinder is then used to measure the excess charge created in the pocket. An electrically-isolated ion probe is inserted into the Gaussian cylinder in order to determine its response in comparison with that of the cylinder.

Exploding-Wire Chamber. The first component downstream from the discharge end of the stagnation chamber is the exploding-wire chamber. It is constructed from a T-shaped copper-pipe fitting with a 7/8-in.-inside diameter. Referencing Fig. 2, page 7, the flow-through portion of the fitting is used to channel the flowstream from the stagnation chamber to the particle separator. The perpendicular portion or neck is used as a portal for inserting the exploding-wire into the flowstream. Referencing Fig. 3, page 9, the wire to be exploded is held in the flowstream by two 3-3/4-in. size-10 copper-wire supports. These two supports are held securely by a machined laminated-phenolic stopper that is inserted into the neck of the copper fitting. The stopper is held in place by an L-shaped clamp which is secured to the neck of the copper fitting by a 1/4-in.-long bolt. The object of the design is easy access for wire changes between firings.

Each of the two size-10 copper-wire supports is held in place in the stopper by a setscrew. One inch of insulation remains on each of the two copper supports and is used as a sleeve for the portion that is routed through the stopper. The setscrews allow the supports to be held securely at any desired height.

The tips of the supports that are inserted into the chamber are

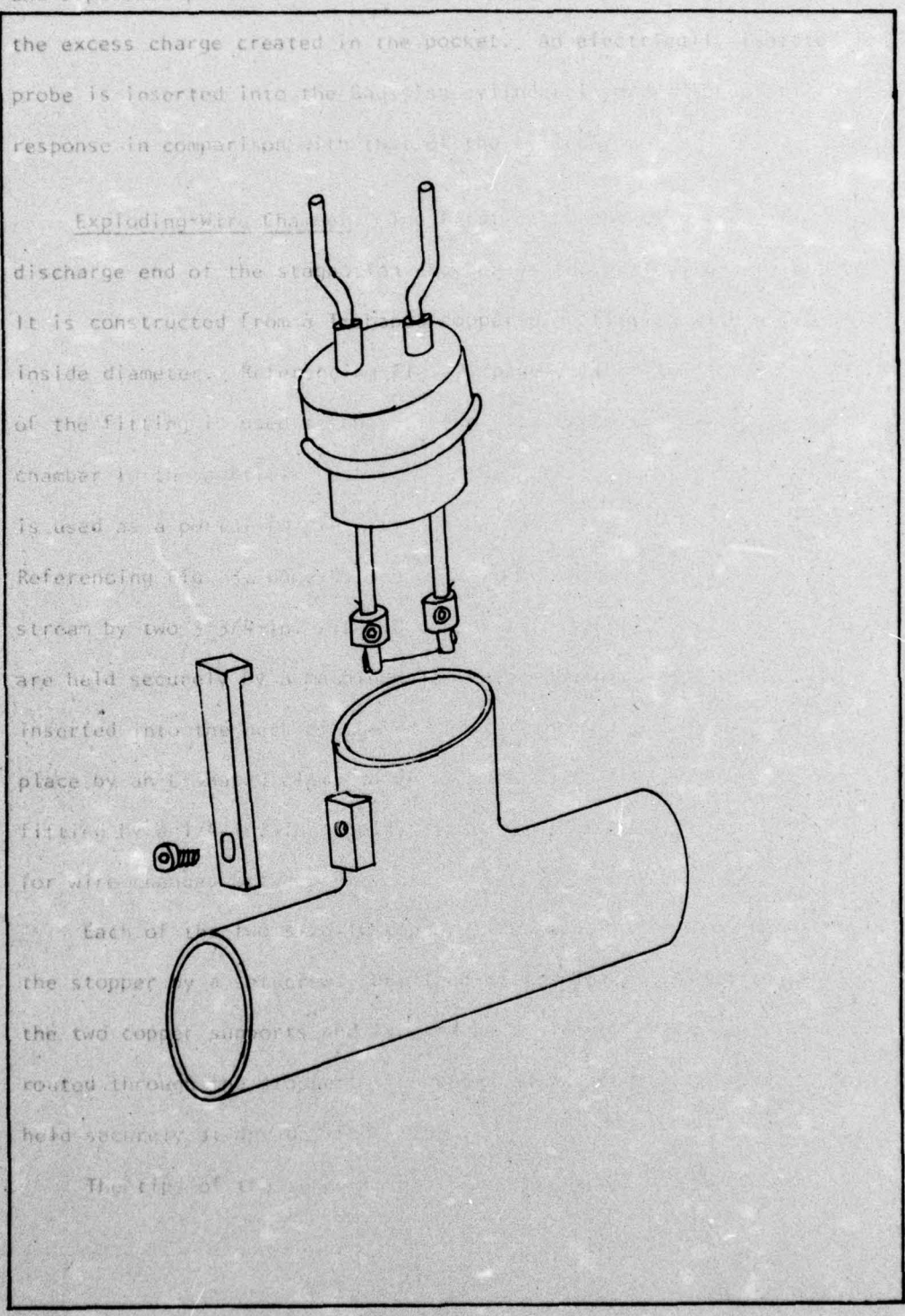

Fig. 3 Exploding-Wire Chamber

filed off flat, notched, and positioned 12 mm apart. The wire to be exploded is placed across the tips in the notches. Each end of the wire is bent so that it lies flat along the surface of its support and is held in place by a 5/16-in.-long, 1/4-in.-diameter sleeve that is tightened with a setscrew. The two ends of the copper supports that extend outside the chamber are the connection points for the capacitive discharge circuit.

Particle Separator. After exiting the exploding-wire chamber, the air flow enters the particle separator. Referencing Fig. 4, page 12, the particle separator is a closed metal box which contains an electrically-isolated turbine blade. The air flow enters the front of the box, impinges on the turbine blade, and then flows out the rear. The particle separator was designed to simulate the separation which takes place within a jet engine. The larger particles strike the blade and/or the inside surface of the box and either richochet a number of times prior to exiting or do not exit at all. The purpose of the design is to allow as many particles as possible to electrically discharge against the metal surfaces.

The sides of the box are constructed of 1/8-in.-thick brass. It is 3-1/2 in. wide, 4-1/2 in. long, and 4 in. high with a 3/8-in.-wide brass flange soldered to both the top and the bottom. The top of the box is a 1/8-in.-thick aluminum plate which is bolted to the top flange with 10 screws. The bottom of the box is constructed from 3/8-in.-thick laminated phenolic in order to keep the turbine blade electrically

isolated from the metal portion of the box. The outside of the bottom of the box is covered with aluminum foil in order to make the particle separator a completely-enclosed metal chamber.

The air flow enters the box through a 2-in.-long, 7/8-in.-diameter brass pipe which is centered on the front face. The flow exits the box through a second pipe with the same dimensions centered on the rear face of the box, 3/4 in. from the top. Air flow Mach values mentioned in this report are measured at this exit.

The turbine blade is fastened to the laminated-phenolic bottom, 1/2 in. from the front face of the box. It is aligned along the centerline of the entrance and exit pipes with its concave surface facing the front of the box. Two 1-in.-long metal bars clamp a flange on the tip of the blade securely to the bottom of the box. The forward bar is held in place with a screw. The rear bar is held in place by a bolt which protrudes through the bottom of the box to the outside. This bolt is used as the electrical pickup point for sensing turbine blade signals. During experimentation, the particle separator is placed in an aluminum-foil-covered cardboard box. The aluminum foil is grounded, shielding the particle separator from stray electrical pickup.

Gaussian Cylinder. After exiting the particle separator, the flowstream enters the Gaussian cylinder. Its purpose is to allow the bolus of charge produced by the particle separator to be measured. The 68-in.-long Gaussian cylinder is constructed from three sections of 7-in.-diameter galvanized pipe. A circular plate with a 2-in.-long, 7/8-in.-

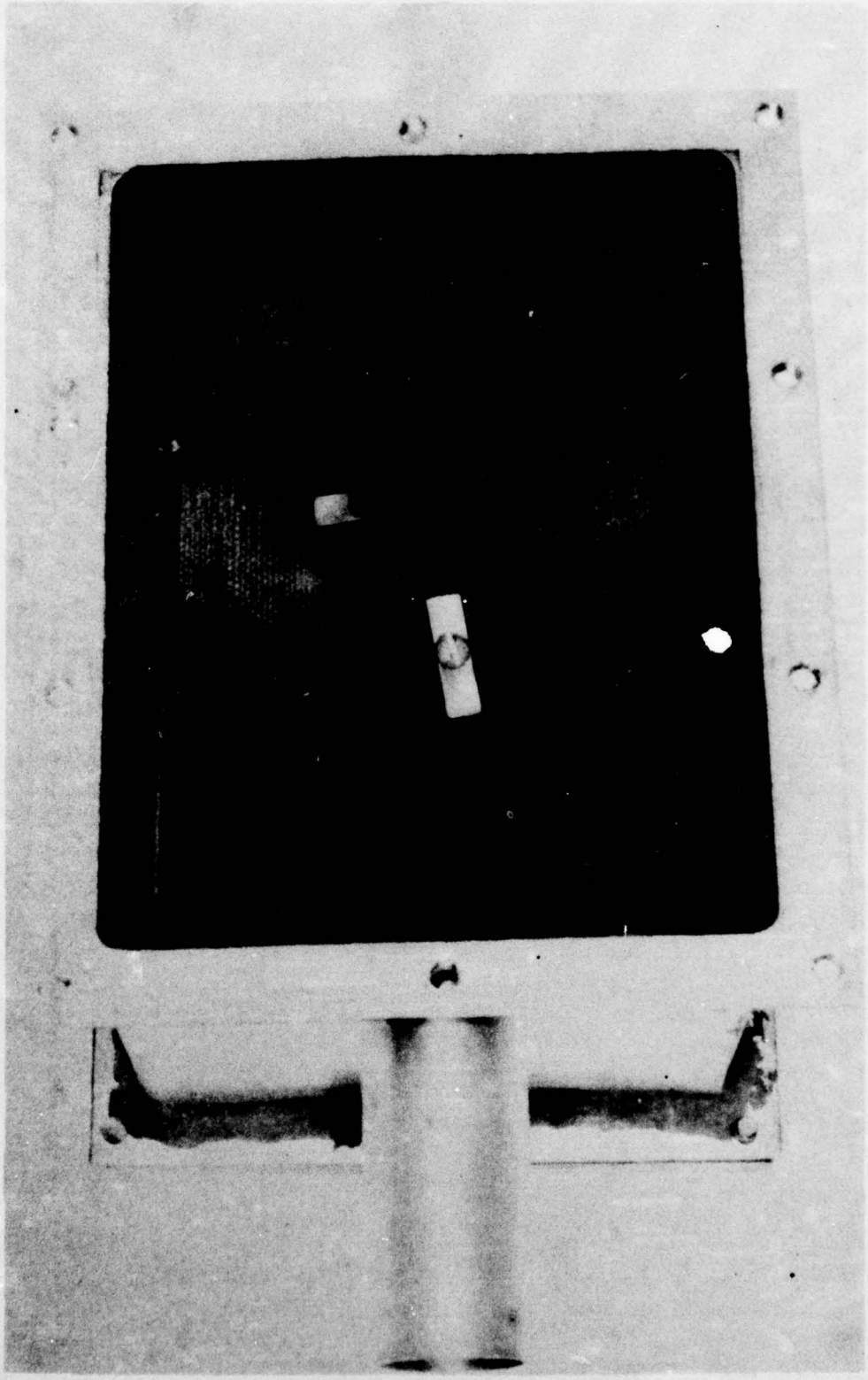

Fig. 4 Particle Separator with Top Removed

diameter copper inflow pipe protruding from its center is soldered onto the front of the cylinder. The rear of the cylinder remains completely open.

An electrically-insulated T-56 ion probe of the type described by Hill (Ref 8:101) is mounted in the side of the Gaussian cylinder. Its shaft is centered across the copper inflow pipe, 2 in. to the rear of the pipe in the interior of the Gaussian cylinder. Its function is to allow ion-probe and Gaussian-cylinder signals to be compared, thereby gaining more information about both the composition of boluses and ion probe responses under varying conditions.

During experimentation, the Gaussian cylinder is covered with a layer of newspaper and a layer of aluminum foil. The aluminum foil is grounded in order to shield the cylinder and the probe from stray electrical pickup.

Exploding-Wire Circuit Elements

Three Sprague CP70E1DJ106X 10-microfarad capacitors are connected in parallel and charged with a Nuclear Research Corporation NS2-A 2500-v power supply. Voltages above 1200 v are measured by a Sensitive Research Instrument Corporation Model ESD electrostatic voltmeter. Below 1200 v, a Systron Donner Model 7000A digital voltmeter is used.

Referencing Fig. 1, page 6, the terminals of the capacitors are connected together with two strips, each consisting of six parallel size-14 copper wires. This design was used in lieu of larger single wires in order to reduce the inductance of the discharge circuit. One

side of the capacitor bank is connected to one of the two exploding-wire supports through a copper throw switch and two 1-in.-lengths of size-10 copper wire. The other side is connected to the other exploding-wire support through a current shunt and two 2-in.-lengths of size-10 copper wire. The current shunt, not shown in Fig. 1, is a shielded tubular shunt of the type described by Park (Ref 13:198-199). The resistance element of the shunt is a 17.5-cm-long tube of type-304 stainless steel with an outside diameter of 0.625 in. and a 0.020 in. wall thickness. Using the handbook resistivity value of 72 microhm-cm for stainless steel, the calculated resistance is 19.5 milliohms.

Both a low resistance and a low inductance in the external circuit are important design factors. The lower the resistance, the higher the partition of energy to the exploding-wire. And the lower the inductance, the shorter will be the time period of the discharge. Referencing Fig. 5a, page 18, the ringing frequency of the circuit, measured by shorting out the exploding-wire supports with size-10 copper wire and discharging the capacitor, is 50 killihertz. The discharge time for the first pulse of current to a wire which is being exploded is 15 microseconds.

Measurement Equipment

Measurements were recorded on Polaroid film with two Tektronix 7904 oscilloscopes. One is equipped with a 7B70 time base and the other with a 7B92 dual time base. Each oscilloscope has two 7-A16A amplifiers which measure a signal across a resistance of 1 megohm. Each oscilloscope also has a C-51 camera and a C-50/C-70 roll film back which uses Polaroid type-47 film.

Signals from the particle-separator box and turbine blade are routed to one oscilloscope with two lengths of RG-62A coaxial cable. Signals from the Gaussian cylinder and ion probe are routed to the other oscilloscope with two additional lengths of RG-62A coaxial cable. Both oscilloscopes are simultaneously triggered externally with a loop of wire around the negative terminal of the discharge circuit.

Limitations

Nichrome V wire is the only type wire used in this research because its composition was the closest match available to that of high-temperature gas-path-component alloys. These alloys contain various combinations of nickel, chromium, and cobalt. Nichrome V wire, however, does not contain cobalt and it is not known what effect its addition would have on the results.

Two different diameters of wire were used: 0.0100 in. and 0.0179 in. The capacitive discharge system is limited to 94 joules by the voltage rating of the capacitors. This is enough energy to partially vaporize the smaller-diameter wire, but only melt the larger one.

Although the air compressor was equipped with a dryer, it was not functioning properly throughout the entire period of this research. Consequently, the magnitude of variations in results due to fluctuations in water-vapor content of the flowstream are unknown. In addition, the air compressor system became contaminated with oil during the latter portion of this research. This contamination, which could not be controlled, altered the experimental results significantly. It is discussed in detail in Section IV.

III. Theory

This section provides a discussion of exploding-wire theory which is augmented with oscilloscope photographs of the current waveform of the capacitive discharge circuit used in this research. An interpretation of oscilloscope signals from the particle separator is given, and the calculation of bolus charge is explained.

Exploding-Wire Theory

Microdistresses were simulated by exploding Nichrome-V wires which are composed of 80 percent nickel and 20 percent chromium. When a wire is exploded, it creates a pocket of hot metal particles, ions, and plasma in varying combinations depending upon the mass of the wire, the energy deposited in that mass, and the circuit discharge time. When energy is delivered to the wire by a capacitive discharge, the wire must be the highest resistance element in the circuit. Through Ohmic heating, the temperature is rapidly raised through its phase points, its melting point, and its vaporization point. Once vaporization begins, usually within a few microseconds after the start of the capacitive discharge, the wire is converted from a conducting liquid to a metallic vapor (Ref 14:519). If the voltage remaining on the capacitor at this point is high enough to electrically break down the metal vapor, current flow continues uninterrupted. If, however, there is insufficient voltage to trigger a breakdown, the current will rapidly decrease to zero. As the metallic-vapor cylinder expands outward and the density decreases,

the voltage required for breakdown becomes lower. If the required breakdown voltage becomes less than the voltage remaining on the capacitor, a restrike occurs and current again flows.

Fig. 5, page 18, shows a sequence of oscilloscope photographs of the waveform of the voltage across the current shunt. Fig. 5a shows the decreasing oscillatory waveform of the discharge circuit when the exploding-wire is shorted out with a length of size-10 wire. Fig. 5b shows the waveform when a 12-mm length of 0.0100-in.-diameter wire is just barely melted with a 750-v discharge. Fig. 5c shows an 1100-v discharge. The small dip in the first hump indicates that vaporization is taking place. The falling of the waveform to zero followed by the formation of a second small hump indicates that a restrike has taken place. Fig. 5d shows a 1200-v discharge during which vaporization takes place, but with sufficient voltage remaining on the capacitor that a restrike occurs before the current drops to zero. Fig. 5e shows vaporization taking place earlier at 1500-v, and with more energy remaining on the capacitor. Fig. 5f shows vaporization occurring even earlier with a 2000-v discharge and with much more energy remaining on the capacitor. The negative portion of the curve indicates that the circuit is beginning to resume its oscillatory characteristic. The peak of 32 v across the 19.5-milliohm shunt resistance element represents a peak current of 1640 amps.

Particle-Separator Signal Interpretation

The particle separator described in Section II, page 10, consists

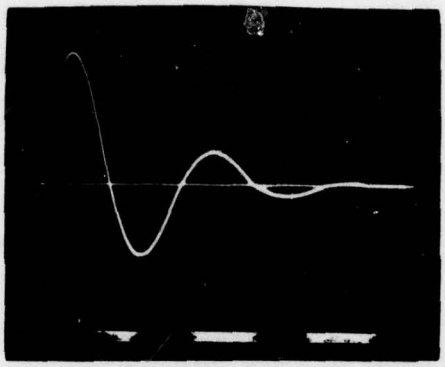

5a. 500-v Capacitor Discharge.

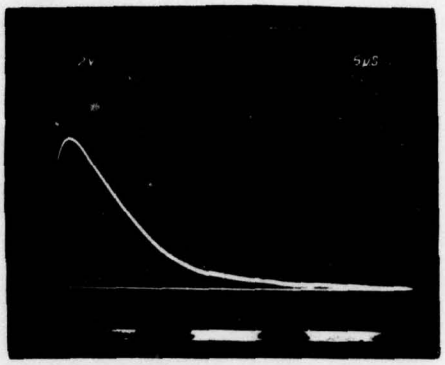

5b. 750-v Capacitor Discharge.

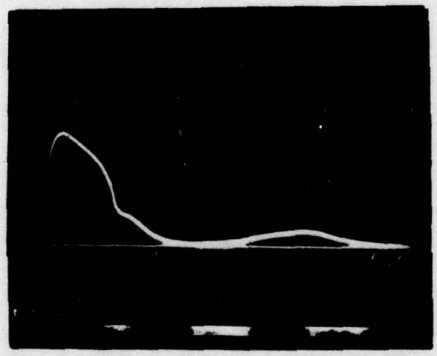

5c. 1100-v Capacitor Discharge.

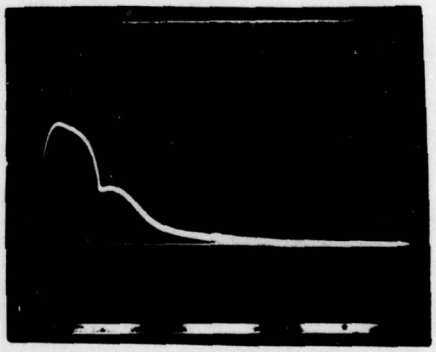

5d. 1200-v Capacitor Discharge.

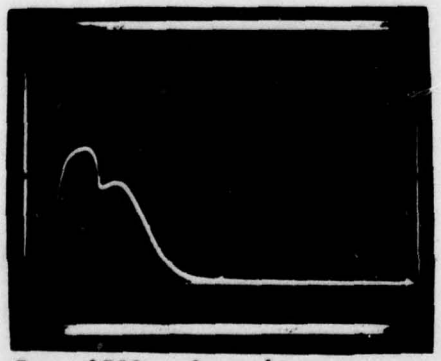

5e. 1500-v Capacitor Discharge.

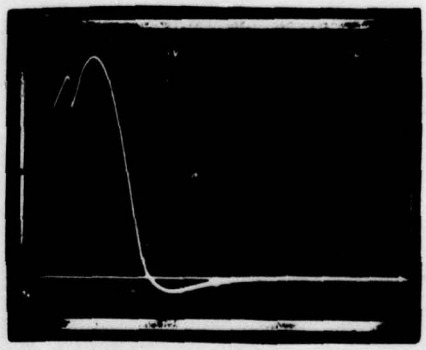

5f. 2000-v Capacitor Discharge.

Fig. 5 Exploding-Wire Current Waveforms for 0.010-in.-Diameter Nichrome-V Wire. Five Volts and 5 Microseconds per Division. Thirty Microfarad Capacitor.

of an electrically-isolated turbine blade mounted in a closed metal box. Signals from the box and the blade are simultaneously measured across 1-megohm resistors by a dual-trace oscilloscope. Fig. 6a below is a photograph of these signals resulting from the explosion of a 12-mm-long, 0.010-in.-diameter, Nichrome wire with a 1000-v discharge and a Mach-1 flowstream exit velocity. Both oscilloscope voltage scales are 5-v per cm and the time scale is 500 microseconds per cm. The top trace is that of the box, the bottom that of the blade.

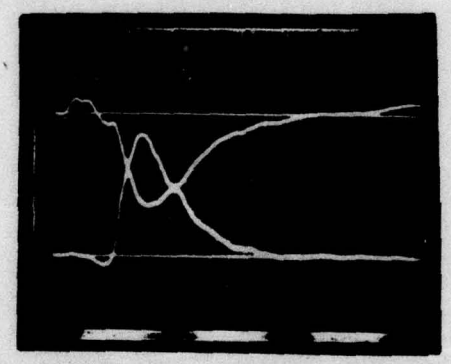

6a. Particle Separator. Top, Box. Bottom, Blade.

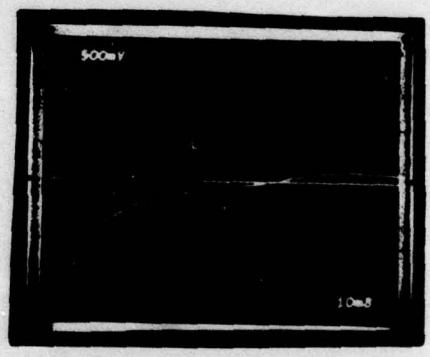

6b. Gaussian Cylinder.

Fig. 6 Oscilloscope Signals from the Explosion of 5.4 mg of 0.0100-In.-Diameter Nichrome-V Wire with a 1000-v Capacitor Discharge

The blade signal shows an initial slight negative dip followed by a large positive peak. This is caused by a leading negative charge being sensed by the blade followed by a positive particle discharge.

Mirrored in time with the positive blade discharge is a negative box peak. Electrons flow from ground to neutralize the positively-charged particles striking the blade. This causes a positive blade signal but because the box is simultaneously gaining negative charge, a negative charge is induced on its outer surface. This induced negative charge flows to ground, causing the box signal. It should be noted that charge transfer between the particles and the inside surface of the box is not detected. This transfer results only in the rearrangement of charge that is already within the box and does not cause more charge to enter.

The box trace also shows a leading induced negative charge followed by an induced positive charge. Note that the initial induced negative point on the blade trace lags the initial negative point on the box trace because the blade is further down the flowstream than the entrance to the box. The box trace begins to go positive after 4 milliseconds. This indicates that a negative charge is leaving the box. Fig. 6b, page 19, is a photograph of the Gaussian cylinder response during the same shot. At the 4-millisecond point, the Gaussian-cylinder waveform shows a negative bolus entering the cylinder. This is the same bolus that is leaving the particle separator in Fig. 6a. Then, Fig. 6b shows the bolus beginning to leave the Gaussian cylinder after 65 milleseconds.

Particle discharges can therefore be distinguished from induced signals in the particle separator by comparing the box and blade signals. A particle discharge is sensed as two waveforms being mirrored in time

but of the opposite sign. An induced signal is sensed as being delayed in time and possibly different in magnitude, but of the same sign.

Bolus Charge Calculation

Fig. 6b, page 19, is an oscilloscope photograph from which the excess charge contained in the bolus can be calculated. As it enters the Gaussian cylinder, the bolus induces an equal amount of charge on the cylinders surface. This charge flows to ground through a 1-megohm resistor in the oscilloscope, resulting in the waveform shown. The total charge Q can be calculated by measuring the area under the curve with a planemeter. A unit square of area on the photograph has the units of volt seconds. However,

$$V = IR \tag{1}$$

and since $R = 10^6$ ohms

$$I = 10^{-6}V \tag{2}$$

or

$$\frac{Q}{t} = 10^{-6}V \tag{3}$$

and

$$Q = 10^{-6}Vt \tag{4}$$

Therefore, if the values for the voltage V and the time t corresponding to 1 unit square of area on the photograph are substituted into equation (4), the bolus charge can be computed by multiplying the right side of the equation by the measured area.

IV. Experimental Results

The purpose of this section is to provide a detailed description, discussion, and evaluation of the experimental results. There were three main areas of investigation: bolus formation, ion-probe response, and bolus charge.

Bolus Formation

The formation of both negatively and positively charged boluses were investigated. Negatively charged boluses were created by the injection of hot metal particles into the flowstream. An investigation of their formation was considered to be of primary importance since a microdistress such as a turbine-blade rub which could lead to catastrophic engine failure would also inject hot metal particles into the flowstream. The understanding of negative-bolus formation therefore appeared to be a key to the prediction of impending jet-engine failures, and therefore the major portion of the investigative effort was made in this area.

Positively charged boluses were created by heating wires to temperatures approaching their melting points. However, time did not permit a full investigation of their mechanism of formation.

Negative Bolus Formation. Figs. 7a and 7b, page 23, show waveforms resulting from the explosion of 5.4 mg of 0.0100-in.-diameter Nichrome-V wire. Fig. 7a shows the particle separator signals. The top trace is from the box, the bottom from the turbine blade. They show initial induced oscillations followed by a very large positive particle discharge.

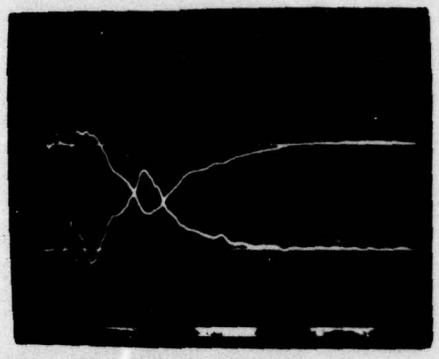

7a. Particle Separator.
Top, Box. Bottom, Blade.

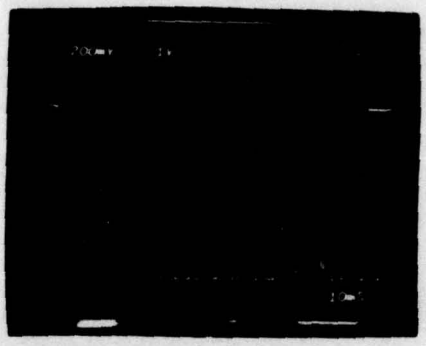

7b. Top, Gaussian Cylinder.
Bottom, Ion Probe.

Fig. 7 Oscilloscope Signals from the Explosion of 5.4 mg of 0.0100-in.-Diameter Nichrome-V Wire with a 2500-v Capacitor Discharge

The very large positive particle discharge was the most prominent feature of all Nichrome-V-wire-explosion particle-separator signals. From this evidence, it was concluded that when a pocket contains hot metal particles, the particles are positively charged.

There is only a slight excess negative charge contained in the pocket prior to its entry into the particle separator. This was confirmed by placing a small Gaussian cylinder between the explosive chamber and the particle-separator. It is not until the particle discharge occurs that the negative bolus is created. This can be seen very clearly in Fig. 8a, page 24. During this shot, the box and blade are electrically bonded together so that the resulting waveform represents the net charge entering or leaving the particle-separator.

Fig. 8a shows an initial negative charge entering followed by a

positive charge. When the particles, the carriers of the positive charge, discharge against the blade the waveform goes very negative. This indicates that negative charge is flowing into the particle-separator through the turbine blade in order to neutralize the positively charged particles. The waveform then goes positive, indicating that the negative bolus which has been created is leaving the particle-separator.

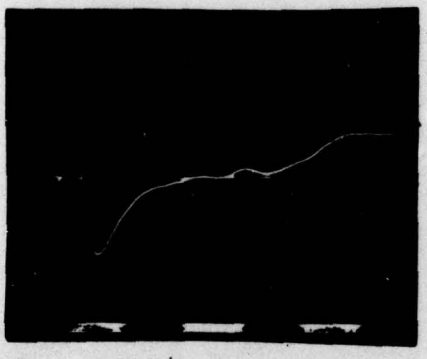

8a. Particle Separator.

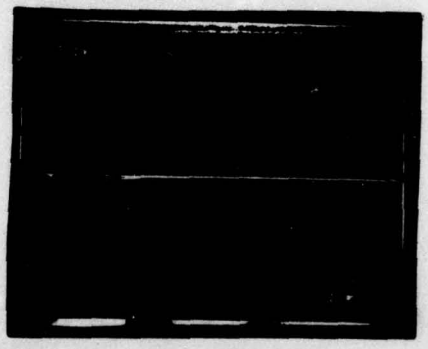

8b. Gaussian Cylinder

Fig. 8 Oscilloscope Signals from the Explosion of 5.4 mg of 0.0100-in.-Diameter Nichrome-V Wire with a 2000-v Discharge. The Box and Blade are Electrically Bonded Together

The exit of the negative bolus is confirmed in Fig. 8b, the Gaussian cylinder trace. It shows a negative bolus entering 3 milliseconds after the wire is exploded. From this evidence, it is concluded that the mechanism for the creation of a negative bolus of charge is either the electrical discharge or separation of the positively-charged metal particles from the pocket. The mechanism for charging the particles is

suspected to be thermionic emission of electrons. An evaluation of this hypothesis is given under the subsection titled Evaluation which begins on page 37.

Gas-Path Microdistress Theory of Bolus Formation. The following theory is suggested by the results described in the preceeding subsection: When a microdistress injects hot metal particles into a flowstream, these particles are positively charged, possibly by thermionic emission. A pocket is created which might be electrically neutral if measured intoto, but is in actuality microscopically composed of separated positively charged particles and negatively charged ions. The pocket follows the flowstream until it is deflected by the first turbine blade or guide vane that it encounters. Here, the ions and very small particles continue to follow the flowstream, but the larger particles are only partially deflected because of their inertia. These larger particles then strike metal flowstream components as they pass through succeeding stages of turbine blades, electrically discharging on contact. The removal of either the positive charge on the particles or the particles themselves is the mechanism for the creation of the negative bolus of charge in the exhaust of a jet engine.

Positive Bolus Formation. Small positive boluses of charge were created by heating a wire with a capacitive discharge. Fig. 9, page 26, shows the waveforms resulting from the heating of a 0.0100-in.-diameter Nichrome-V wire with a 600-v discharge. The wire can be melted

with a 650-v discharge. The basic particle-separator configuration was used with an exit velocity of Mach 1.

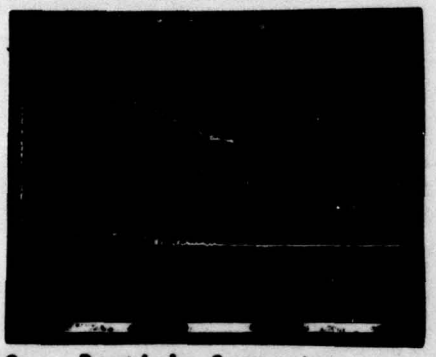

9a. Particle Separator. Top, Box. Bottom, Blade.

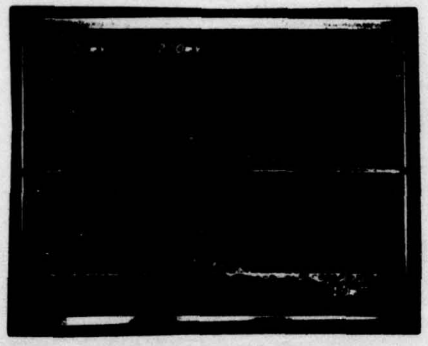

9b. Top, Gaussian Cylinder. Bottom, Ion Probe.

Fig. 9 Positive Bolus Waveforms

The top trace in Fig. 9a is from the particle-separator box. The bottom trace is from the particle-separator turbine blade. Both show positive waveforms, indicating that no large particle discharge is occurring. The top trace of Fig. 9b is that of the Gaussian cylinder which shows a positive 12-nanocoulomb bolus of charge. The top scale is 200 mv per cm and the bottom scale is 20 mv per cm. The bottom trace is that of the ion probe which also has a positive waveform.

Time did not permit an investigation of the mechanism for positive bolus creation. However, both the rapid oxidation of the hot metal surface or the emission of positively charged metal ions are possible candidates. The oxidation of a metal surface increases with temperature.

And if negative oxygen ions were to be drawn from the air to the metal surface, a positive excess charge would be left in the air. The emission of positively charged metal ions would add positive charge to the gas stream.

Regardless of the mechanism, however, this gives insight into the creation of positive boluses of charge within an engine. A microdistress which would cause the overheating of a surface without the injection of metal particles into the flowstream could result in the creation of a positive bolus of charge.

Boluses from Copper and Carbon. A shot with copper wire resulted in the same particle-separator and Gaussian-cylinder waveforms that had been obtained with Nichrome-V wire. However, a shot with carbon pencil lead resulted in the waveforms shown in Fig. 10 below.

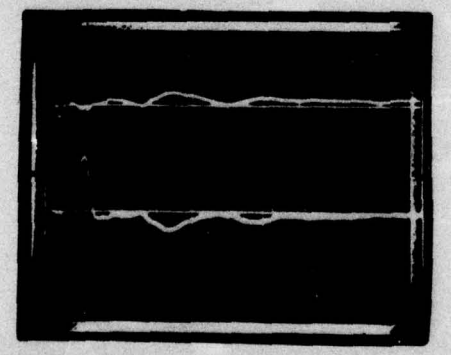

10a. Particle Separator. Top, Box. Bottom Blade.

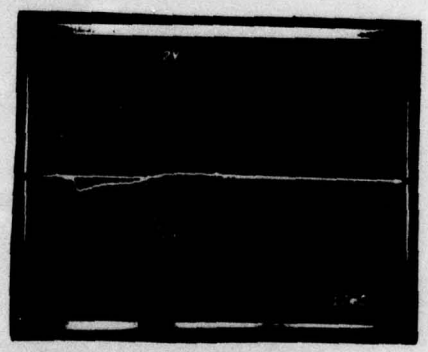

10b. Gaussian Cylinder.

Fig. 10 Oscilloscope Signals from the Explosion of Carbon Pencil Lead

The carbon pencil lead was 0.5 mm in diameter. Fig. 10a shows a small negative particle discharge to the turbine blade. Fig. 10b shows that the resulting bolus was negative. These results indicate that carbon particles may become negatively charged if they are present during a microdistress. Experimentation with carbon was not continued since time did not permit. Therefore, a theory to explain this result is not proposed. It should be noted, however, that carbon (pencil lead) did not produce a significant amount of excess charge and hence, it is expected that soot boluses would not be highly charged.

Ion-Probe Response

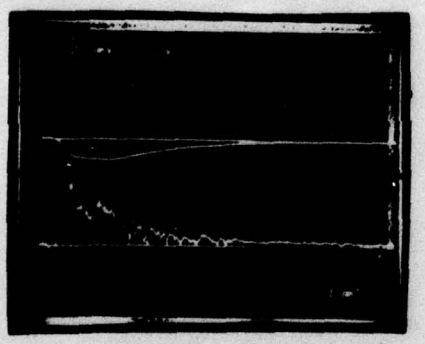

11a. Top, Gaussian Cylinder. Bottom, Ion Probe. No Steel Wool.

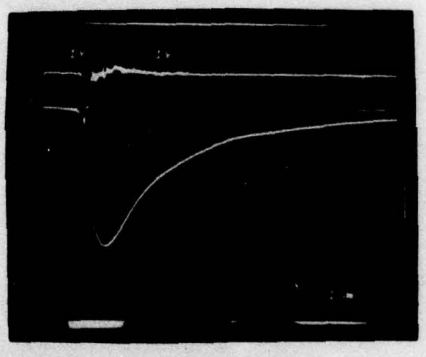

11b. Top, Ion Probe. Botton, Gaussian Cylinder. Steel Wool in Box.

Fig. 11 Comparison of Normal Ion-Probe and Gaussian Cylinder Responses

Normal Ion-Probe Response. The bottom trace of Fig. 11a, page 28, shows the typical ion-probe response to a negative bolus entering the Gaussian-cylinder at an exit velocity of Mach 1 from the particle separator. The capacitor voltage was 2000 v and 5.4 mg of 0.0100-in.-diameter Nichrome-V wire was exploded. The top trace of Fig. 11a shows the corresponding Gaussian cylinder response. The top voltage scale is 2 v and the bottom scale is 200 millivolts. Note that although the excess of charge of the bolus is clearly negative as indicated by the Gaussian-cylinder response, the ion-probe response shows a small leading negative signal followed by a large-area positive signal. In the absence of the Gaussian-cylinder information, one would probably interpret the ion-probe response as sensing a positively charged bolus. The difference between the two responses can be explained if the negative bolus still contains very small positively charged particles that were not separated by the particle-separator. Apparently this is the case, since placing steel wool in the particle separator for better separation results in the ion-probe signal shown in the top trace of Fig. 11b. In this shot, 5.4 milligrams of 0.0100-in.-diameter Nichrome-V wire was exploded with a 2200 v discharge. The bottom trace is the corresponding Gaussian-cylinder signal. Note that in this case there is a very large initial negative peak that decays rapidly into a shallow positive peak. The waveform of the ion-probe here approximates the derivative of the Gaussian cylinder waveform as it should for an induced signal. From this evidence, it must be concluded that when charged particles are

present in a bolus, induced ion-probe signals are masked by particle discharge signals.

Contaminated Ion-Probe Response. The reversal of the normal response was experienced after the ion-probe surface became contaminated with exploding-wire combustion products. The surface contamination occurred as a result of unintentional contamination of the flowstream components with oil from the air compressor.

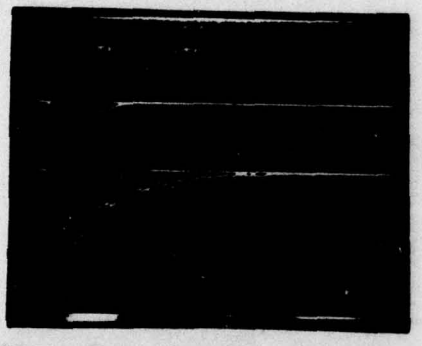

12a. Top, Gaussian Cylinder. Bottom, Ion Probe. Contaminated Probe.

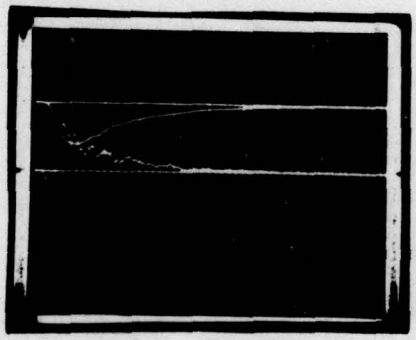

12b. Top, Gaussian Cylinder. Bottom, Ion Probe. Clean Probe

Fig. 12 Responses of an Exploding-Wire-Combustion-Product-Contaminated Ion Probe and a Clean Ion Probe

The two photographs in Fig. 12 show the ion-probe and Gaussian-cylinder signals from two successive explosions of 5.4 mg of 0.0100-in.-diameter Nichrome-V wire at 2200 v. Steel wool was not used in the particle-separator and the flowstream exit velocity was Mach 1. The

bottom trace of Fig. 12a shows the response of the contaminated probe. There are small positively charged particles in the bolus, yet the contaminated probe shows a large area negative discharge. The bottom trace of Fig. 14b shows the probe response after its surface has been cleaned with acetone. The response is normal.

It should be noted that the Gaussian-cylinder responses show a decrease in bolus charge between the uncontaminated and contaminated shots. There are two possible explanations: either the positively charged particles become even more positively charged with surface contact with the contaminated probe or negative ions are discharging to the surface of the probe. It is believed that the partial discharge of the negative bolus to the combustion-product contaminated surface of the probe is the more likely explanation.

Ion-probe signal distortion of a second type was also discovered during the period of oil contamination. When the surface of the probe was rubbed with an oil-contaminated paper filter taken from the entrance of the stagnation chamber upstream from the explosion chamber, the positive large area portion of the probes waveform was eliminated.

Both photographs in Fig. 13, page 32, were taken during the explosion of 5.4 mg of 0.0100-in.-diameter Nichrome-V wire with a 2000 v discharge. Steel wool was not used in the particle separator and the exit velocity was Mach 1. The top trace in Fig. 13 a shows the ion-probe response after its surface was rubbed with the oil-contaminated filter paper. This resulted in the elimination of the large area portion

of the normal probe signal. The top trace of Fig. 13b shows the response of the probe after its surface was cleaned with acetone. The response is normal. Oil contamination apparently prevents charged

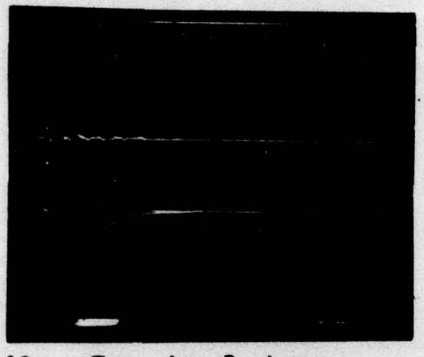

13a. Top, Ion Probe. Bottom, Gaussian Cylinder. Contaminated Probe.

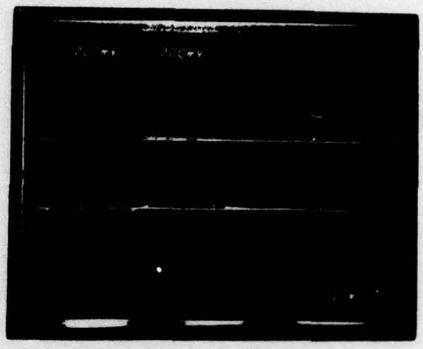

13b. Top, Ion Probe. Bottom, Gaussian Cylinder. Clean Probe.

Fig. 13 Responses of an Oil-Contaminated Ion Probe and a Clean Ion Probe

particles from discharging to the surface of the probe. Note that the waveform of the contaminated probe response in Fig. 13a looks very similar to the response of a probe to a bolus which is formed with steel wool in the particle separator such as shown in the top trace of Fig. 11b, page 28. When steel wool is used virtually all of the particle discharge has been eliminated because the particles themselves have been separated from the bolus much more efficiently by the steel wool.

Measurement of Bolus Charge

Results. A series of shots was taken with 0.0100-in.-diameter Nichrome-V wire in order to measure the amount of charge produced versus capacitor voltage. The capacitor discharge voltage was varied between 800 v and 2400 v. The particle-separator exit velocity was Mach 1. An average of 5.4 mg was exploded in each shot. The basic turbine-blade and box configuration of the particle-separator was used without steel wool. The bottom curve in Fig. 15, page 38, shows the resulting nanocoulomb-versus-voltage plot.

After the series of measurements was made, the air-compressor system and the apparatus became contaminated with oil, causing large decreases in resulting bolus charges. But when grade-3 coarse steel wool was placed in the particle separator behind the blade and in the exit pipe, the resulting boluses were even larger than had been previously created. After placing clean steel wool in the box, the first shot would always cause a very large bolus. But the second and third shots with the same steel wool would result in boluses that were much reduced in charge. Succeeding shots would produce boluses with only approximately half the charge contained in the bolus created with the first shot. Two possible causes of the bolus charge reduction were the contamination of the steel wool by the oil itself or contamination by exploding-wire combustion products which were present as a result of the oil contamination. The first possibility was checked by allowing the air to flow through clean steel wool for three cycles prior to

making a shot. This did not cause a reduction in bolus charge. The second possibility was contemplated after noting that the exploding-wire supports were often covered with a sooty deposit following a shot. Discoloration of the steel wool in the exit-pipe was also observed at the same time. A series of shots was taken after changing only the exit pipe wool in the particle separator. This resulted in the same phenomenon of a very large bolus of charge for the first shot and a large decrease in charge during succeeding shots. It was therefore concluded that the presence of oil during the wire explosion caused contamination of the steel wool with combustion products.

The decrease in charge resulting from the two types of contamination, oil and combustion-product, resulted from two different mechanisms as was pointed out in the subsection titled Contaminated Ion-Probe Response which begins on page 28. The oil coating on the metal surfaces inside the particle-separator simple prevented the particles from discharging as efficiently. When steel wool was not used, the negative bolus still contained fine positively charged particles. However, with the use of steel wool, virtually all of these particles were removed. Therefore the increase in bolus charge with the use of steel wool is the result of a better particle discharge and separation efficiency. The use of steel wool remedied the reduction in efficiency caused by the failure of the small particles to discharge against the oil-contaminated inside surfaces of the particle separator.

This explanation, however, does not account for the reduction in

charge in succeeding shots using the same wool. The negative bolus is created by the elimination of the positive charge carried by the particles. Whether elimination occurs through electrical discharge or particle separation should make no difference. Therefore, if all the particles are being separated with steel wool, some other mechanism which affects the negative ions in the bolus must be responsible for the charge reduction. It is therefore believed that the combustion-product contamination causes a partial discharge of the negative bolus itself. This hypothesis is strengthened by the observation of a combustion-product contaminated probe described on pages 30 and 31.

After the contamination effects were fully explored, runs with 0.0100-in. and 0.0179-in.-diameter wires were made with steel wool in the particle separator. At each capacitor discharge voltage, three shots were made. Fresh steel wool was placed in the particle-separator exit pipe for the first shot of each series of three shots. The succeeding two shots were made with the same wool. The ion-probe and Gaussian-cylinder responses recorded in two of these three-shot series are shown in Fig. 14, page 36. The left voltage scale value shown at the top of each photograph refers to the Gaussian-cylinder trace which is on the bottom. The right voltage scale value refers to the top trace, that of the ion probe. The objective of these shots was to plot a maximum and minimum charge-versus-voltage curve for each diameter wire using steel wool and compare them with the results of a previous series of shots which was made before the oil contamination occurred. It was hypothesized that the curve obtained

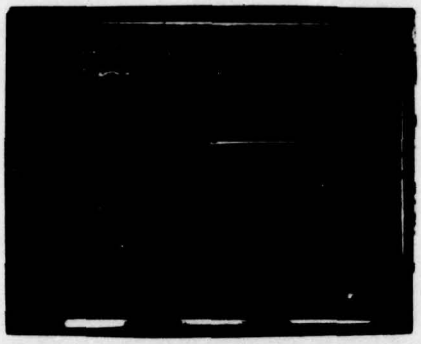

14a. First Shot, 5.4 mg.
385 nanocoulombs.

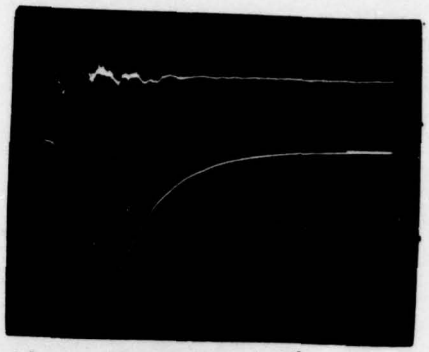

14d. First Shot, 16 mg.
340 nanocoulombs.

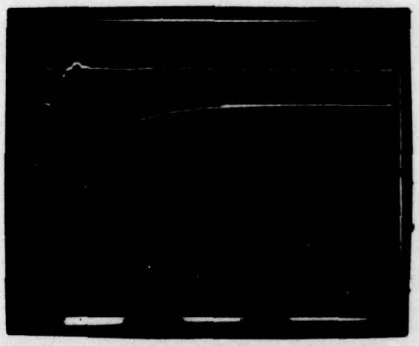

14b. Second Shot, 5.4 mg.
155 nanocoulombs.

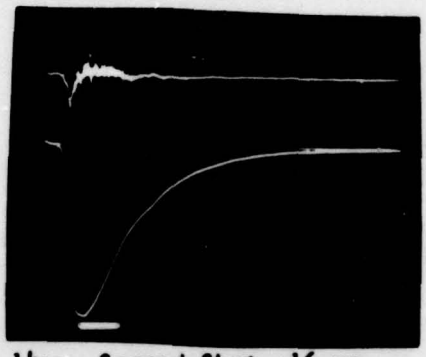

14e. Second Shot, 16 mg.
240 nanocoulombs.

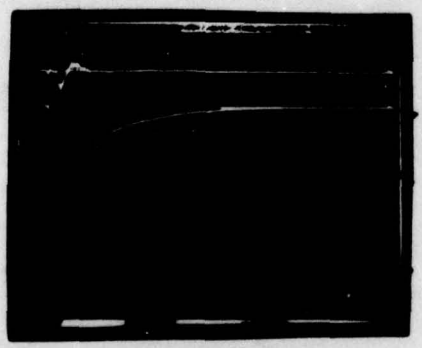

14c. Third Shot, 5.4 mg.
145 nanocoulombs.

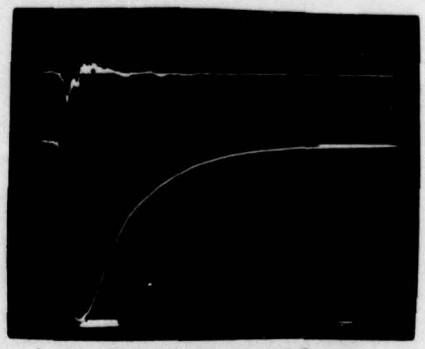

14f. Third Shot, 16 mg.
220 nanocoulombs.

Fig. 14 Oscilloscope Signals from Two 3-Shot Series with 5.4 mg of 0.0100-in. and 16 mg of 0.0179-in.-Diameter Nichrome-V Wire. Top Trace is Ion Probe. Bottom Trace is Gaussian Cylinder. Capacitor Discharge 2500 v for 0.0100-in. and 2300 v for 0.0179-in.-Diameter Wires.

using the first-shot values with steel wool should approximate the maximum bolus charge attainable since all the particles were being separated and the combustion-product contamination would not be present to discharge the negative bolus. The other curves should have the same shape, but lower values, and would represent lower charge-separation efficiencies. Figures 15 and 16 on pages 38 and 39 show the resulting curves. The top two curves in each figure are the results of the shots with steel wool. The bottom curve in each figure is a series without steel wool. For the 0.0100-in.-diameter wire, the series without steel wool was taken before the oil contamination problem occurred. All shots with the 0.0179-in.-diameter wire were taken after the oil contamination. Note that the maximum charge values with steel wool were always obtained on the first shot for the high discharge voltages, and the minimum charge values occurred predominantly but not solely on the third shot.

Evaluation. In order to compare the amount of charge observed with that expected from the thermionic emission model developed in Appendix B, it is necessary to make estimates of the average particle size, emission time, and temperature.

Baker and Warchal (Ref 2:218) found that when 0.060-in. and 0.030-in.-diameter zirconium wires were exploded, the largest diameter particles were obtained at the lowest temperatures and were initially 1.33 times the wire diameter. At higher energies, approximately 100 microns was the smallest average diameter obtained. Assuming that these values are reasonable for Nichrome-V wire, 300-micron-diameter particles

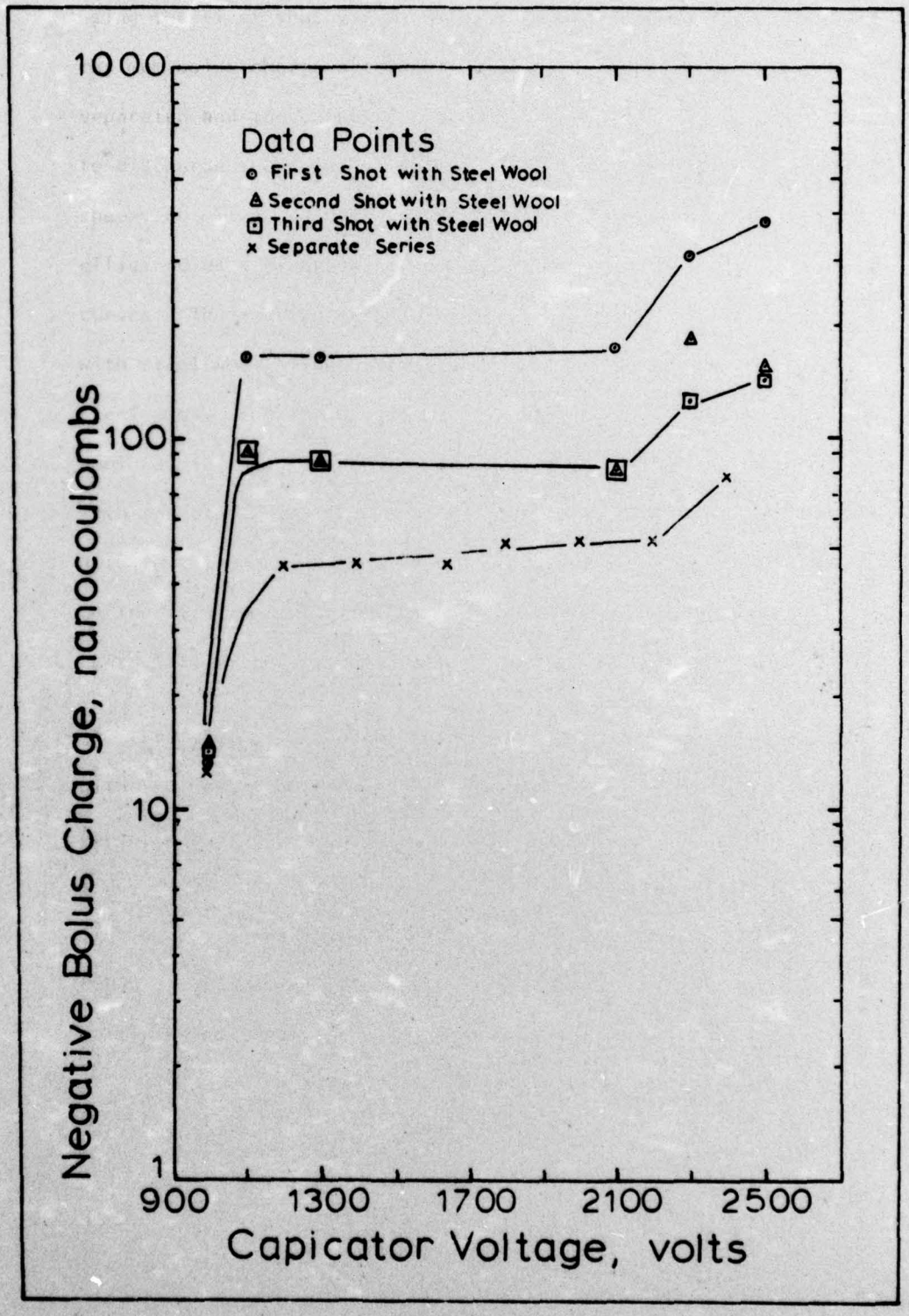

Fig. 15 Negative Bolus Charge Vs. Discharge Voltage for 5.4 mg of 0.100-In.-Diameter Nichrome-V Wires

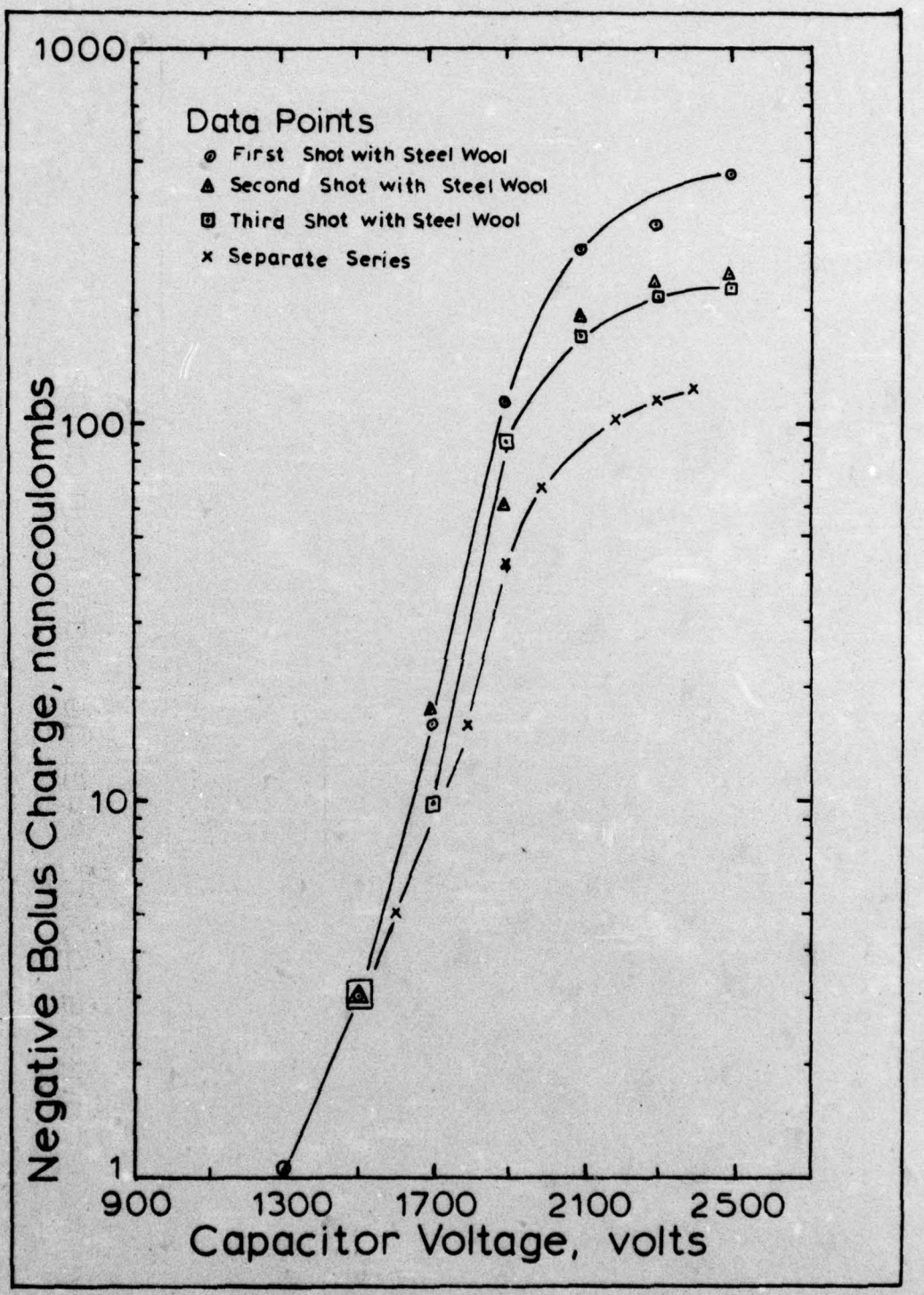

Fig. 16 Negative Bolus Charge Vs. Discharge Voltage for 16 mg of 0.0179-In-Diameter Nichrome-V Wires

could be expected from 0.0100-in.-diameter wire and 500 micron diameter particles could be expected from 0.0179 in. diameter wire at lower temperatures just above the melting point.

An average emission time can be approximated from the observation that molten metal droplets splatter onto the turbine blade in the particle separator. From Fig. 7a, page 23, the peak particle discharge to the turbine blade occurs after 1.25 milliseconds has elapsed. A reasonable temperature estimate would be 2000°K which lies between the melting points of nickel and chromium.

Using these three estimates, assuming that 300-micron and 500-micron-diameter particles emit electrons for 1.25 milliseconds at 2000°K, Figures 19 and 20, pages 54 and 55, show that 75 and 125 nanocoulombs would be the maximum charge expected from thermionic emission of exploded 0.0100-in. and 0.0179-in.-diameter Nichrome-V wires, respectively. This is a much higher value, however, than the 1 to 5 nanocoulombs that have been measured at discharge voltages which will just barely melt the wire. But when one checks the maximum possible charge on the assemblage of particles given by Figures 17 and 18, pages 50 and 51, 1.1 and 2 nanocoulombs are the maximum possible for 300-micron and 500-micron-diameter particle assemblages. This agrees very well with the values of charge actually measured at the lower temperatures. Therefore, corona discharge probably limits the amount of charge on a particle at the lower temperatures before it can attain that value expected from thermionic emission.

To account for the maximum charge values of 385 and 460 nanocoulombs which have been measured at the highest discharge voltages for 0.0100-in. and 0.0179-in.-diameter wires, one must enter Figures 17 and 18 with an assumed average particle size on the order of 20 microns. With this assumed particle size, the graphs predict that 200 and 575 nanocoulombs of charge are the maximum values possible without corona discharge. In order to get the observed maximums of 385 and 460 nanocoulombs, the average particle diameter would have to be slightly less than 20 microns for 0.0100-in.-diameter wire and slightly more for 0.0179-in.-diameter wire. This is reasonable since the 0.0100-in.-diameter wires were heated to hotter temperatures and therefore smaller particles could be expected. Additionally, it should be noted that the maximum-charge-versus-diameter curves on pages 50 and 51 are not linear. The presence of a very few small particles would cause an assemblage to be able to hold more charge than that value indicated for the average diameter. Therefore, if a number of particles with less than 10 microns diameter were present, the same maximum charge values could be attained with an average assemblage diameter greater than 20 microns.

At the higher temperatures, the charge is also limited by corona discharge. To check the charge expected from thermionic emission against the maximum possible due to carona discharge, a conservative assumption is made that at 2800°K a 20-micron-diameter particle assemblage emits during the second half of the 15-microsecond circuir discharge time. Fig. 19, page 54, predicts that 22,500 nanocoulombs would be produced from thermionic emission. This value is probably high because

of the assumption in the calculations discussed in Appendix B that the emitting material is grounded and therefore electrons are replaced as they are emitted. There are only 9 coulombs of charge available from stripping an electron from the outer shell of each atom in 5.4 milligrams of 0.0100-in.-diameter Nichrome-V wire. But even though the 22.500 nanocoulomb value is high, it is still far above the 200 nanocoulomb limit predicted for 0.0100-in.-diameter wire due to corona discharge.

It is concluded that the values of bolus charge measured during this research are well below the values that are possible by thermionic emission and are on the order of the maximum possible on a particle due to corona discharge. Therefore, thermionic emission is a possible explanation for the observed positive charge on the particles.

V. Conclusions and Recommendations

The purpose of this section is to summarize the important conclusions which have been reached and to make recommendations for changes to the current jet-engine monitoring procedures based upon the results of this research.

Conclusions

Negative Bolus Formation Theory. The following theory is suggested by the experimental results: When a microdistress injects metal particles into a flowstream, these particles are positively charged, possibly from thermionic emission of electrons from their surfaces. A pocket is created which might be electrically neutral if measured intoto, but is microscopically composed of separated positively charged particles and negatively charged ions. The pocket follows the flowstream until it is deflected by the first turbine blade or guide vane that it encounters. Here, the ions and very small particles continue to follow the flowstream, but the larger particles are only partially deflected because of their inertia. These larger particles stike metal flowstream components as they pass through succeeding stages of turbine blades, electrically discharging on contact. The removal of either the positive charge on the particles or the particles themselves is the mechanism for the creation of a negative bolus of charge in the exhaust of a jet engine.

Positive Bolus Formation. Positive boluses of charge were created by heating a wire to a temperature near its melting point. However,

the resulting charge was an order of magnitude smaller than the charge created in a negative bolus by exploding the same length of wire. Time did not permit an investigation of the mechanism for the formation of positive boluses. Regardless of the mechanism, however, this information is useful as insight into the creation of positive boluses of charge within a jet engine. A microdistress which would cause the overheating of a surface without the injection of metal particles into the flowstream would result in the creation of a positive bolus of charge.

Ion-Probe Response. The response of an ion probe can be very unreliable. When particles are contained in a bolus, their discharge to the ion probe surface will mask the ion induced waveform. Oil contamination of an ion-probe has been shown to inhibit particle charge transfer. Contamination by exploding-wire combustion products is believed to have caused negative-ion discharge to a probe surface. Therefore, when used as a sole source of information, an ion probe can give very misleading information as to the actual charge in a bolus. However, when used in conjunction with a Gaussian cylinder as was done in this research, it can provide reliable information about the particle content of a bolus.

Recommendations

Ion-Probe Equipment Augmentation. Ion-probe responses have been shown to be very misleading when they are the sole source of information.

It is therefore recommended that the ion probes which are currently used to monitor jet engines be augmented by additional equipment based on the Gaussian-cylinder principle. A number of designs would be possible. The most obvious would be to place a large electrically-insulated cylinder behind the engine. A second possibility would be to electrically-insulate the tail pipe and use it as a Gaussian cylinder. A third possibility would be to spray or place an electrically insulated conducting surface on the inside of the tail pipe. A fourth possibility might be to place a number of rings of electrically-isolated buttons on the inside of the tail pipe and connect them together for use as one sensor.

The Importance of Negative-Bolus Detection. This research has shown that negative boluses indicate the presence of hot metal particles. Since hot metal particles would most probably be produced by a micro-distress which would result in catastrophic engine failure, immediate attention should be given to negative-bolus detection.

Hardware designed on the Gaussian-cylinder concept could be used to detect negative boluses. A coincidence circuit could be designed to accept the inputs of an ion probe and a Gaussian cylinder. It would trigger on the synchronized receipt of a large leading negative cylinder signal and a positive probe signal. To insure reliability, however, a study of ion-probe signal distortion due to surface contamination by jet engine exhaust may have to be performed.

Bibliography

1. Arlen, Richard E. An Investigation of Laser-Target Interaction Signals. Unpublished Thesis. Wright-Patterson Air Force Base, Ohio: Air Force Institute of Technology, December 1975.

2. Baker, Louis Jr. and Raymond L. Warchal. "Studies of Metal-Water Reactions by the Exploding Wire Technique." Exploding Wires, 2:207-233 (1962).

3. Burgess, Ray W. An Investigation of the Detection of Charged Metal Particles in a Jet Engine Exhaust by a Cylindrical Electrostatic Probe. Thesis, AD745540. Wright-Patterson Air Force Base, Ohio: Air Force Institute of Technology, June 1972.

4. Cassady, John T. Effect of Simulated Turbine on Airflows Carrying Charged Particles. Unpublished Thesis. Wright-Patterson Air Force Base, Ohio: Air Force Institute of Technology, May 1975.

5. Couch, Robert P., et al. "Sensing Incipient Engine Failure." Progress in Astronautics and Aeronautics, 34:515-529 (1972).

6. Driver-Harris Company Technical Bulletin No. 159. Thermoelectric Properties and Design Data for Temperature Measurements. Harriston, N. J.: Driver Harris Company, 1959.

7. Fowler, R. T. Ion Collection by an Electrostatic Probe in a Jet Exhaust. Thesis, AD874647. Wright-Patterson Air Force Base, Ohio: Air Force Institute of Technology, June 1970.

8. Hill, Gail E. Imminent Engine Failure Probe Investigation. AFAPL TR-74-30. Wright-Patterson Air Force Base, Ohio: Air Force Aero Propulsion Laboratory, 1974.

9. Labo, Jack A. The Theory of an Electrostatic Metal-Particle Sensor Operating in a Jet Engine Exhaust. Thesis, AD768351/9. Wright-Patterson Air Force Base, Ohio: Air Force Institute of Technology, June 1973.

10. Kittel, Charles. Introduction to Solid State Physics. New York: John Wiley and Sons. 1960.

11. Lapple, C. E., et al. Advances in Chemical Engineering. New York: The Academic Press. 1970

12. Mitchell, Donald A. and Frederick C. Bauer. Evaluation of an Electrostatic Probe Technique for Detection of Turbine Engine Gas Path Distress, Comprehensive Summary Report. AFAPL TR-74-96. Wright-Patterson Air Force Base, Ohio: Air Force Aero Propulsion Laboratory, 1975.

13. Park, John H. "Shunts and Inductors for Surge-Current Measurements." Journal of Research of the National Bureau of Standards, 39:191-212 (September 1947).

14. Sacks, R. D., and J. A. Holcombe. "Radiative and Electrical Properties of Exploding Silver Wires." Applied Spectroscopy, 28: 518-535 (November/December 1974).

Appendix A

Maximum Charge of a Small Particle

The atmospheric breakdown potential at sea level is approximately 3 v/micron (Ref 11:44). This is true, however, only for a uniform field such as exists between two flat plates. In order to achieve breakdown, electrons must be able to accelerate sufficiently within their mean free paths to ionize air molecules. Since the field between two parallel plates is uniform, the acceleration is the same at any point in the field. The field of a spherical body, however, decreases in proportion to the square of the distance from its center. And the smaller the body, the greater its curvature and the more rapidly the electric field intensity decreases within the distance of a mean free path of an electron from its surface. Lapple (Ref 11:26) has calculated the positive-corona threshold limits for spherical particles. The values range from 250 v/micron for 10-micron-diameter particles to 9 v/micron for 1000-micron-diameter particles. Using lapple's values, Figures 17 and 18, pages 50 and 51, give the maximum charge versus particle size for 0.0100-in. and 0.0179-in.-diameter wires. Fig. 17 assumes the complete conversion of 5.4 mg 0.0100-in.-diameter wire into spherical particles of a single diameter and gives the maximum theoretical charge on the assemblage. Fig. 18 makes the same assumption for 16 mg of 0.0179-in.-diameter wire.

The values for the maximum charge Q for a particle of radius r are calculated from the formula

$$E = \frac{Q}{4\pi\varepsilon_o r^2}$$

where E is the maximum field strength given by Lapple, and $\varepsilon_o = 8.845 \times 10^{-12}$ F/m.

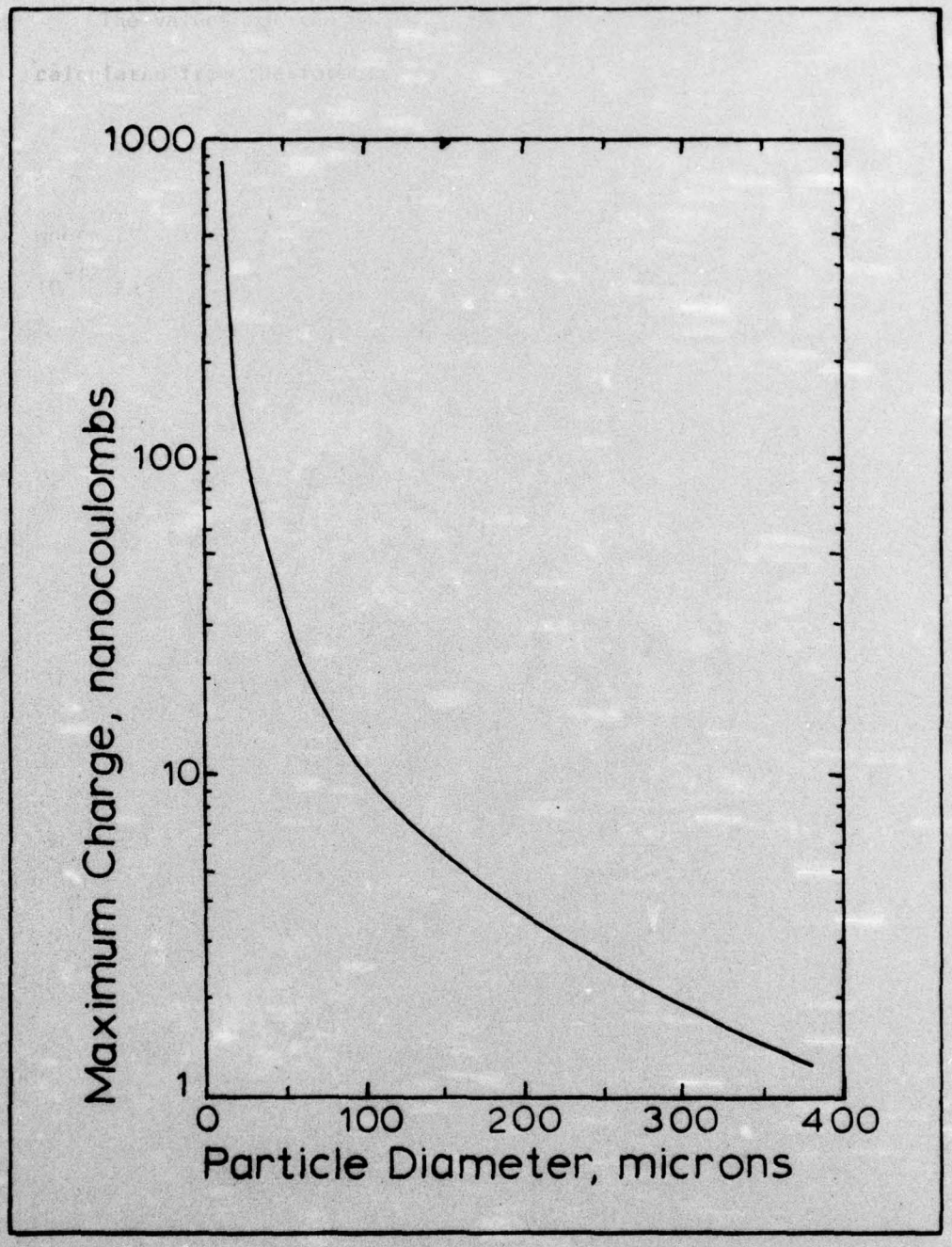

Fig. 17 Theoretical Maximum Charge Vs. Particle Diameter for 5.4 mg of 0.01-in.-Diameter Nichrome-V Wire Converted to Spherical Particles

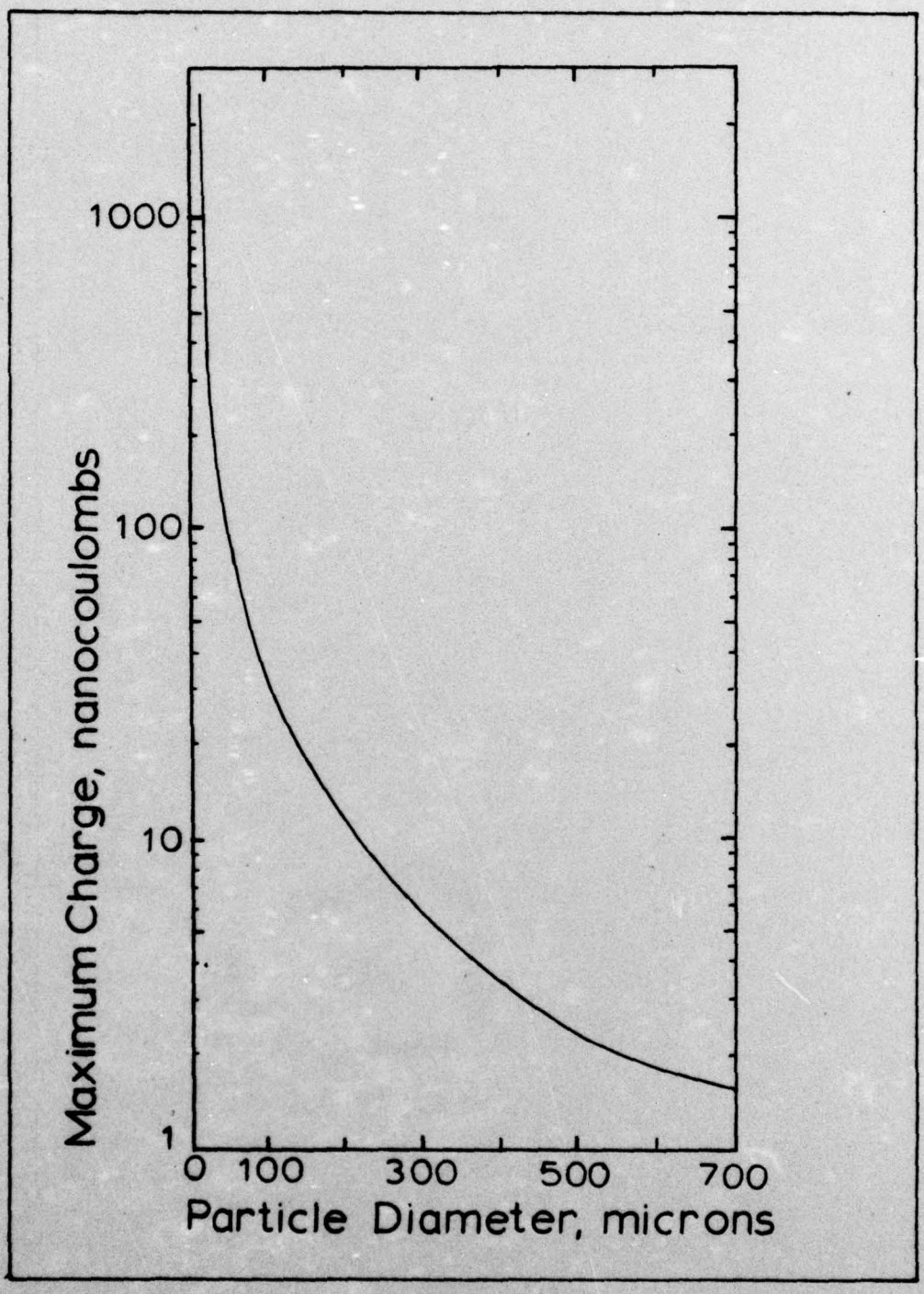

Fig. 18 Theoretical Maximum Charge Vs. Particle Diameter for 16 mg of 0.0179-in.-Diameter Nichrome-V Wire Converted to Spherical Particles

Appendix B

Thermionic Emission

The purpose of this appendix is to calculate a theoretical order-of-magnitude maximum for the amount of charge possible from thermionic emission of electrons from the surface of an assemblage of metal particles formed during the wire explosions of this research.

Electrons are thermionically emitted from a surface when it is heated. The Richardson-Dushman equation gives an expression for the resulting current density J as

$$J = AT^2 e^{-\phi/kT} \qquad (6)$$

where the constant A and the work function ϕ for nickel and chromium are given in Table I below. A weighted average for the constant A has been computed for Nichrome-V wire. T is the temperature in degrees Kelvin and kT is the electron temperature in electron volts (ev) where 1 ev equals 11,600 degrees Kelvin (Ref 10:267).

Table I

Richardson-Dushman Equation Constants

Metal	A(amp/cm^2 $^\circ$K^2)	ϕ ev	Melt Pt. $^\circ$K	Vapor Pt. $^\circ$K
Ni	30	4.6	1726	3005
Cr	48	4.6	2130	2945
.8 Ni + .2 Cr	33.6	4.6	1670	3000 Est.

When a wire is exploded, the initial temperature of the resulting particles can vary between the melting and boiling points of the wire. The melting point of Nichrome-V wire given by the Driver-Harris Company is approximately 1670 °K, which is close to the melting point of Ni (Ref 6:12). The vaporization temperature was not available. However, assuming that it approximates the vaporization temperature of Ni, initial particle temperatures in the range from 1700 °K to 3000 °K are possible.

Figures 19 and 20, pages 54 and 55, show the theoretical currents predicted by the Richardson-Dushman equation for 0.0100-in. and 0.0179-in.-diameter Nichrome-V wires in the temperature range of 1700 °K to 3000 °K. These curves assume an average exploded mass of 5.4 mg for 0.0100-in. wires and 16 mg for 0.0179-in.-diameter wires and that the entire mass is converted to spherical droplets of the same diameter. The current density J in the Richardson-Dushman equation has been multiplied by the total surface area of the assemblage of sperical particles in order to obtain the current which is plotted in Figures 19 and 20.

It should be noted that in the derivation of the Richardson-Dushman equation, it was assumed that the emitted electrons were instantaneously replaced in the metal by other electrons from ground. This is obviously not the case for isolated particles. The emission of electrons from a particle without replacement would cause an increase in the height of the potential well with a resulting decrease in the emission current density. This effect has not been compensated for in the charts and would cause a decrease in the calculated charge.

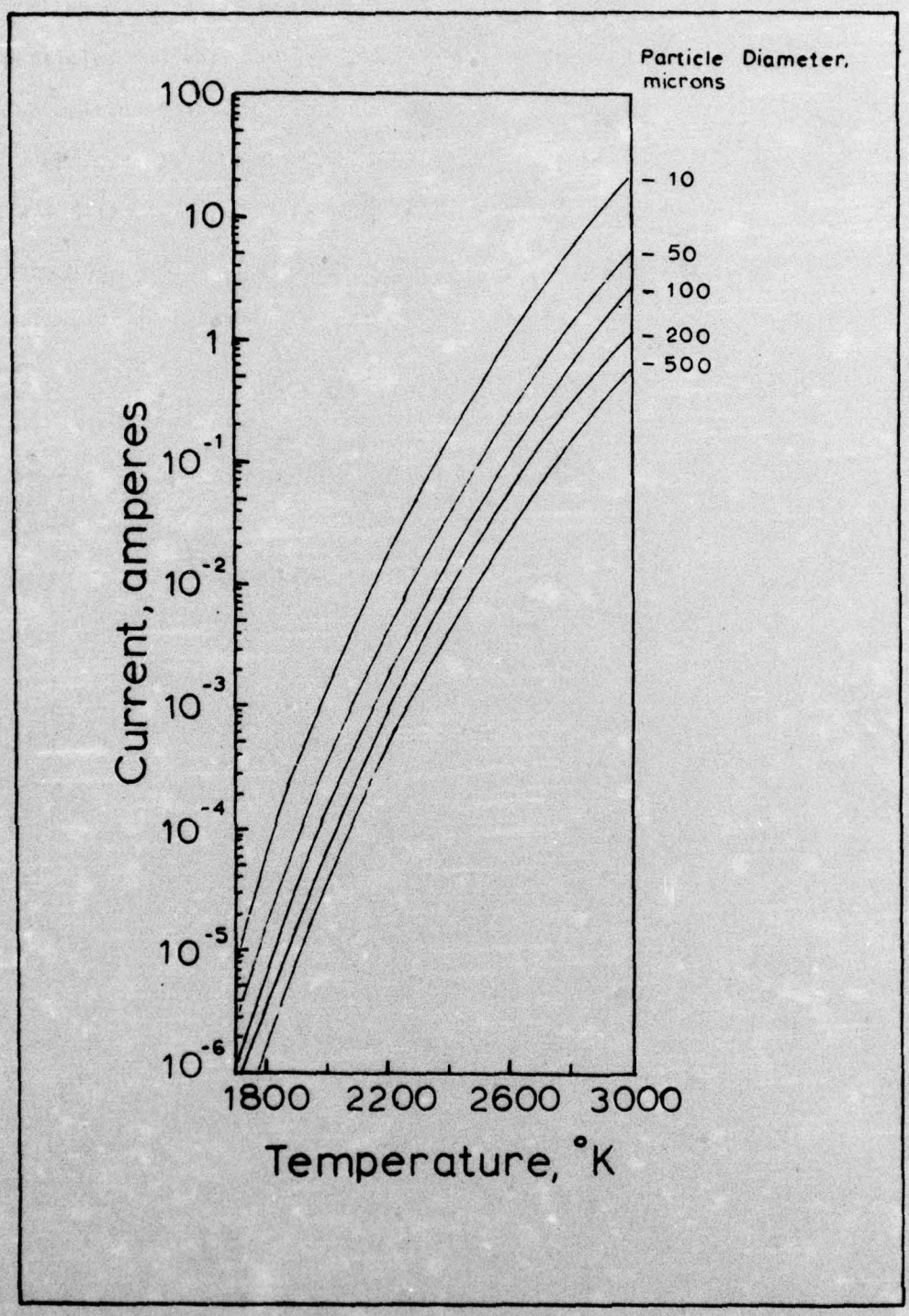

Fig. 19 Theoretical Thermionic Emission Current Vs. Temperature for Various Particle Sizes for 16 mg of 0.0179-in.-Diameter Nichrome-V Wire Completely Converted to Spherical Particles

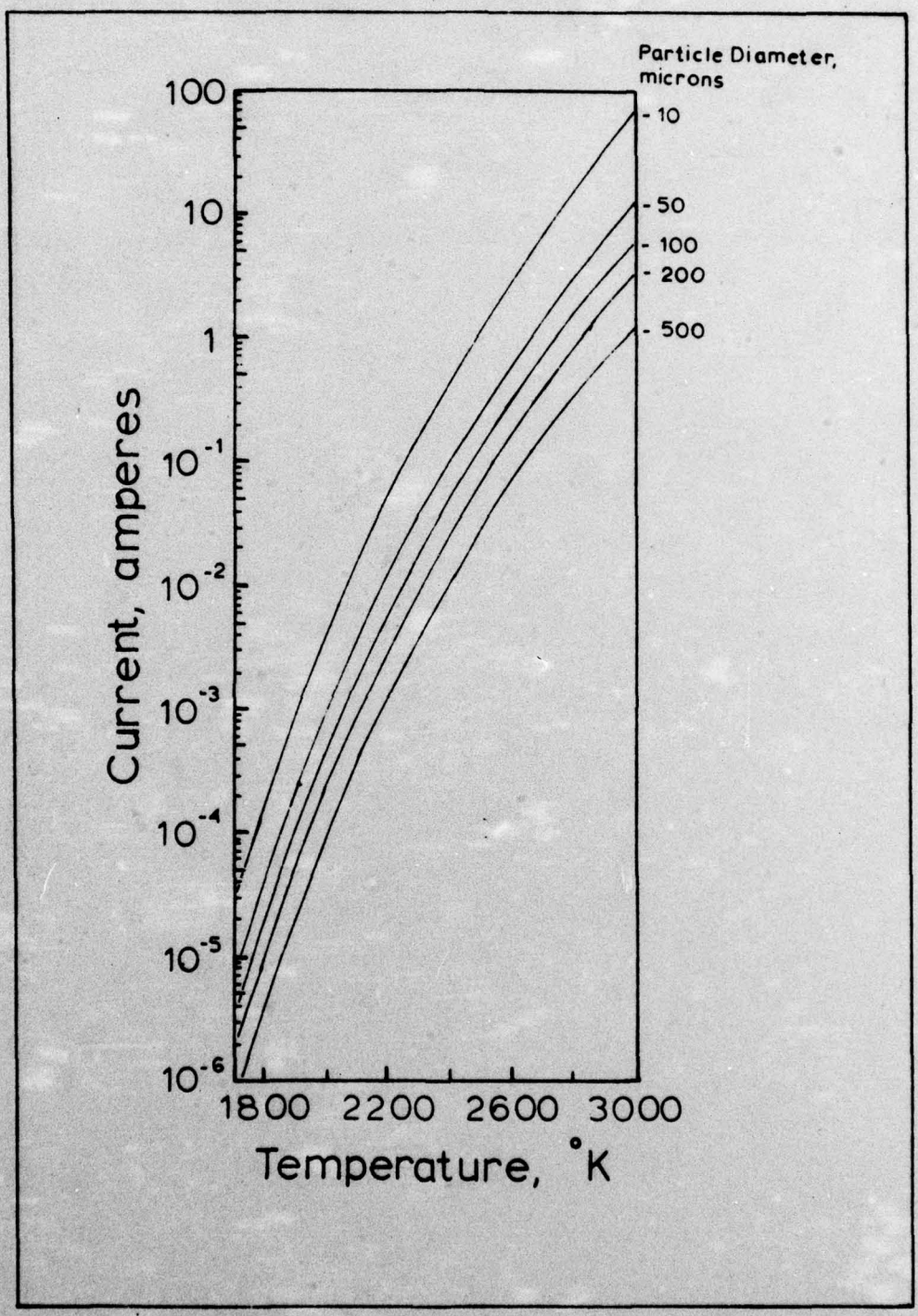

Fig. 20 Theoretical Thermionic Emission Current Vs. Temperature for Various Particle Sizes for 16 mg of 0.0179-in.-Diameter Nichrome-V Wire Completely Converted to Spherical Particles

To use the charts to compute the maximum possible charge from thermionic emission, an average temperature, an average particle size, and an average emission time must be assumed. The current is determined from the chart by entering with the temperature and particle size. The charge is then computed by multiplying the current by the emission time.

Vita

John Esca Mitchell was born on 31 October, 1939 in Abingdon, Virginia. He graduated from Spring Garden High School in Chatham, Virginia in 1956 and attended Virginia Polytechnic Institute from which he received the degree of Bachelor of Science in Physics in 1961. After completing Pilot Training at Laredo AFB, Texas in July 1962, he spent four years flying C-124 aircraft at Hunter AFB, Georgia, and four years flying C-141 aircraft at McGuire AFB, New Jersey. He was Flying Safety Officer for the 438th Military Airlift Wing at McGuire AFB for 2 years prior to going to Vietnam in 1971. In Vietnam, he was stationed at Binh Thuy AB as an advisor to the Chief of Safety of the 4th Vietnamese Air Division, where he flew A-37 aircraft with the Vietnamese Air Force and was awarded the Distinguished Flying Cross and the Air Medal with five Oak Leaf Clusters. Upon his return to the United States, he served as Chief of Flying Safety for the 60th Military Airlift Wing at Travis AFB, California until entering the School of Engineering, Air Force Institute of Technology, in June 1974.

Permanent address: Spring Garden
Chatham, Virginia 24531

UNCLASSIFIED

SECURITY CLASSIFICATION OF THIS PAGE (When Data Entered)

REPORT DOCUMENTATION PAGE		READ INSTRUCTIONS BEFORE COMPLETING FORM
1. REPORT NUMBER GNE/PH/75-20	2. GOVT ACCESSION NO.	3. RECIPIENT'S CATALOG NUMBER
4. TITLE (and Subtitle) EXPLODING WIRE SIMULATION OF JET-ENGINE GAS-PATH MICRODISTRESSES		5. TYPE OF REPORT & PERIOD COVERED MS Thesis 6. PERFORMING ORG. REPORT NUMBER
7. AUTHOR(s) John E. Mitchell Major USAF		8. CONTRACT OR GRANT NUMBER(s)
9. PERFORMING ORGANIZATION NAME AND ADDRESS Air Force Institute of Technology (AFIT-EN) Wright-Patterson AFB, Ohio 45433		10. PROGRAM ELEMENT, PROJECT, TASK AREA & WORK UNIT NUMBERS
11. CONTROLLING OFFICE NAME AND ADDRESS Air Force Flight Dynamics Laboratory (AFFDL-FGL) Wright-Patterson AFB, Ohio 45433		12. REPORT DATE December, 1975 13. NUMBER OF PAGES 57
14. MONITORING AGENCY NAME & ADDRESS(if different from Controlling Office)		15. SECURITY CLASS. (of this report) Unclassified 15a. DECLASSIFICATION/DOWNGRADING SCHEDULE

16. DISTRIBUTION STATEMENT (of this Report)

Approved for public release; distribution unlimited.

17. DISTRIBUTION STATEMENT (of the abstract entered in Block 20, if different from Report)

18. SUPPLEMENTARY NOTES

Approved for public release; IAW AFR 190-17

JERRAL F. GUESS, Captain, USAF
Director of Information

19. KEY WORDS (Continue on reverse side if necessary and identify by block number)

Exploding Wires	Exhaust Gases	Ions
Failure	Simulators	Charged Particles
Jet Engines	Flow	Metals
Predictions	Jets	Powder Metals
Probes	Electrostatic Fields	

20. ABSTRACT (Continue on reverse side if necessary and identify by block number)

Exploding wires were used to simulate jet-engine gas-path microdistresses. The physical processes involved in the formation of boluses of charge in a flowstream were investigated and the amounts of bolus charge produced under various conditions were measured. Ion-probe responses were concurrently recorded. The results of the investigation were used to construct a theory of bolus formation.

DD FORM 1 JAN 73 1473 EDITION OF 1 NOV 65 IS OBSOLETE

UNCLASSIFIED

SECURITY CLASSIFICATION OF THIS PAGE (When Data Entered)

Large negative boluses of charge were produced by the injection of hot metal particles into a flowstream. Smaller positive boluses were produced by heating a wire to a temperature near its melting point. Ion-probe responses were shown to be very misleading when used as a sole source of information as to the charge in a bolus. It is recommended that immediate attention be given to the detection of negative boluses of charge in a jet engine exhaust since negative boluses would most probably be produced by the more severe (very hot particles) microdistress which could lead to catastrophic engine failure.